Massive calcium–activated endocytosis without involvement of classical endocytic proteins

Vincenzo Lariccia, Michael Fine, Simona Magi, Mei-Jung Lin, Alp Yaradanakul, Marc C. Llaguno, and Donald W. Hilgemann

Department of Physiology, University of Texas Southwestern Medical Center at Dallas, Dallas, TX 75390

We describe rapid massive endocytosis (MEND) of >50% of the plasmalemma in baby hamster kidney (BHK) and HEK293 cells in response to large Ca transients. Constitutively expressed Na/Ca exchangers (NCX1) are used to generate Ca transients, whereas capacitance recording and a membrane tracer dye, FM 4–64, are used to monitor endocytosis. With high cytoplasmic adenosine triphosphate (ATP; >5 mM), Ca influx causes exocytosis followed by MEND. Without ATP, Ca transients cause only exocytosis. MEND can then be initiated by pipette perfusion of ATP, and multiple results indicate that ATP acts via phosphatidylinositol-bis 4,5-phosphate (PIP_2) synthesis: PIP_2 substitutes for ATP to induce MEND. ATP-activated MEND is blocked by an inositol 5-phosphatase and by guanosine 5′-[γ-thio]triphosphate (GTPγS). Block by GTPγS is overcome by the phospholipase C inhibitor, U73122, and PIP_2 induces MEND in the presence of GTPγS. MEND can occur in the absence of ATP and PIP_2 when cytoplasmic free Ca is clamped to 10 µM or more by Ca-buffered solutions. ATP-independent MEND occurs within seconds during Ca transients when cytoplasmic solutions contain polyamines (e.g., spermidine) or the membrane is enriched in cholesterol. Although PIP_2 and cholesterol can induce MEND minutes after Ca transients have subsided, polyamines must be present during Ca transients. MEND can reverse over minutes in an ATP-dependent fashion. It is blocked by brief β-methylcyclodextrin treatments, and tests for involvement of clathrin, dynamins, calcineurin, and actin cytoskeleton were negative. Therefore, we turned to the roles of lipids. Bacterial sphingomyelinases (SMases) cause similar MEND responses within seconds, suggesting that ceramide may be important. However, Ca-activated MEND is not blocked by reagents that inhibit SMases. MEND is abolished by the alkylating phospholipase A_2 inhibitor, bromoenol lactone, whereas exocytosis remains robust, and Ca influx causes MEND in cardiac myocytes without preceding exocytosis. Thus, exocytosis is not prerequisite for MEND. From these results and two companion studies, we suggest that Ca promotes the formation of membrane domains that spontaneously vesiculate to the cytoplasmic side.

The Journal of General Physiology

INTRODUCTION

Experiments demonstrating that Ca influx triggers exocytosis of neurotransmitters are a cornerstone of modern physiology (Katz, 1996). Recently, the regulatory roles of Ca in endocytic responses, occurring subsequent to exocytosis, have gained attention. One common observation is that progressively larger Ca transients trigger progressively larger endocytic responses, resulting in "excessive" endocytosis, such that cell area decreases below basal levels (Thomas et al., 1994; Smith and Neher, 1997; Engisch and Nowycky, 1998). In melanotrophs, 25% of the cell surface can be internalized in a few seconds after release of caged Ca (Thomas et al., 1994). These responses occur in the absence of cytoplasmic potassium, a condition in which clathrin-dependent endocytosis is blocked (Ivanov, 2008) by disruption of adapter protein 2 (AP2) complexes (Altankov and Grinnell, 1995). Furthermore, the vesicles generated can be larger than expected for clathrin-mediated endocytosis (Thomas et al., 1994). In synapses, endocytic mechanisms that appear to be related to "excessive" endocytosis become dominant as synaptic activity increases. Dubbed "bulk endocytosis," this form of scaffold-independent endocytosis is evidently controlled and/or driven by dynamins (Clayton and Cousin, 2009). That Ca influx through Ca channels can trigger endocytosis is also well established in non-excitable cells, such as oocytes (Vogel et al., 1999). A general biological response involving Ca-activated endocytosis is the response of cells to membrane ruptures or "wounding" (Idone et al., 2008). In brief, punctures of the cell surface flood cells with Ca, and such membrane wounds are closed by fusion of internal membranes with the cell surface, followed by

Correspondence to Donald W. Hilgemann: donald.hilgemann@utsouthwestern.edu

Abbreviations used in this paper: AMP-PNP, adenylyl imidodiphosphate; AP2, adapter protein 2; BEL, bromoenol lactone; BHK, baby hamster kidney; BMCD, β-methylcyclodextrin; EDA, ethylenediamine; GTPγS, guanosine 5′-[γ-thio]triphosphate; HPCD, hydroxypropyl-β-cyclodextrin; HRP, horseradish peroxidase; MEND, massive endocytosis; NTA, nitrilotriacetic acid; PIP_2, phosphatidylinositol-bis 4,5-phosphate; SMase, sphingomyelinase.

The Rockefeller University Press $30.00
J. Gen. Physiol. Vol. 137 No. 1 111–132
www.jgp.org/cgi/doi/10.1085/jgp.201010468

removal of "lesion" membrane by endocytosis (Idone et al., 2008) to non-acidified membrane compartments (Cocucci et al., 2004).

Calmodulin and Ca/calmodulin-dependent phosphatases have been suggested repeatedly to play crucial roles in the actions of Ca to promote endocytosis in secretory cells (Artalejo et al., 1996; Engisch and Nowycky, 1998; Marks and McMahon, 1998; Chan and Smith, 2001; Wu et al., 2009). Inhibition by specific inhibitors of calcineurin (Engisch and Nowycky, 1998; Marks and McMahon, 1998) provides clear evidence for a role of this phosphatase, a role that may reflect regulation of dynamin 1 by its dephosphorylation (Smillie and Cousin, 2005). However, other reagents used to implicate calmodulin are less specific. Cationic peptides used to "block calmodulin" (Wu et al., 2009) bind phosphatidylinositol-bis 4,5-phosphate (PIP_2) with high affinity (de Haro et al., 2004), and the use of calmodulin antibodies to define calmodulin-dependent processes (Artalejo et al., 1996) has not yet been demonstrated to be reliable or specific.

We describe here efforts over several years to understand how large Ca transients cause massive endocytosis (MEND) responses in baby hamster kidney (BHK) fibroblasts, HEK293 cells, and cardiac myocytes. During these studies, it became apparent that Ca promotes MEND by long-term effects that can accumulate over multiple Ca transients, as well as by short-term mechanisms that require the immediate presence of cytoplasmic Ca. To our surprise, we were not able to implicate any classical endocytic protein in MEND, including clathrin, dynamins, and actin cytoskeleton, whereas it became increasingly clear that the membrane itself (e.g., its cholesterol content) strongly influences MEND. Thus, we were forced to consider how mechanisms inherent to the membrane itself might be important.

From several possibilities, ceramide metabolism appeared of interest. Bacterial sphingomyelinases (SMases), which generate ceramide from sphingomyelin, cause large endocytic responses in ATP-depleted macrophages and fibroblasts (Zha et al., 1998) and cause giant liposomes to bud vesicles to the membrane side opposite to which they are applied (Holopainen et al., 2000). This type of endocytosis reflects the formation of ceramide domains that develop high inward curvature and undergo spontaneous budding and fission (Goñi and Alonso, 2009; Staneva et al., 2009). As described here, exogenous SMases can indeed cause MEND within seconds. However, Ca-activated MEND is not caused by the exocytosis of SMases and ceramides, as suggested in a study published since this article was first submitted (Tam et al., 2010). Rather, MEND can be dissociated from exocytosis by pharmacological means, and MEND occurs in some cell types without detectable exocytosis. Furthermore, MEND is not blocked by cell treatments that are described to disrupt acid SMase activities. We suggest that Ca-activated MEND may rather reflect the coalescence of previously existing lipid domains, followed by their spontaneous budding and fission to the cytoplasmic side.

As an orientation to our presentation of Results, we describe first electrical and optical data demonstrating that MEND represents endocytosis rather than membrane shedding, and that membrane proteins are internalized. Equivalent results are presented as supporting data for two other MEND protocols. Second, we describe the existence of two different forms of Ca-activated MEND. Third, we describe five different protocols that induce Ca-dependent MEND, followed by salient observations made with each protocol. Fourth, we describe MEND responses induced by bacterial SMases and evidence that the exocytosis of SMases does not mediate Ca-activated MEND. Finally, we describe Ca-activated MEND that occurs in cardiac myocytes without preceding exocytosis.

MATERIALS AND METHODS

Cell culture, NCX1–pHluorin fusion, and myocyte

BHK cells expressing NCX1.1 (Linck et al., 1998) were maintained as described previously (Yaradanakul et al., 2007). T-REx-293 cells (Invitrogen) were stably transfected with pcDNA3.1 (+) to express an NCX1.1 fusion with a pH-sensitive green protein, pHluorin (Miesenböck et al., 1998), near the NCX1 glycosylation site (Hryshko et al., 1993). Cells were grown in DMEM (Mediatech, Inc.) with 10% (wt/vol) FBS, 2 mM L-glutamine, 100 U/ml penicillin, and 100 µg/ml streptomycin. T-REx-293 cells were selected with G418, Zeocin, and Blasticidine, and transfections were with Lipofectamine 2000 (Invitrogen). Cells were harvested at 80–90% confluency with trypsin (0.25%). Cardiac myocytes were isolated as described previously (Yaradanakul et al., 2007) and used within 3 h.

Generation of the NCX1–pHluorin fusion near the NCX1 glycosylation site

The pcDNA3.1 (+) NCX1.1 (available from GenBank/EMBL/DDBJ under accession no. L06438) plasmid (provided by J.P. Reeves, University of Medicine and Dentistry of New Jersey, Newark, NJ) was mutagenized using a QuickChange Site-Directed Mutagenesis kit (Agilent Technologies) to include a novel ClaI restriction site near to the glycosylation site, using the primers 5′-GCTCTCTT-GTTTTCCCATATCGATGTGGACCATATAAGTGC-3′ and 5′-GCA-CTTATATGGTCCACATCGATATGGGAAAACAAGAGAGC-3′. pHluorin cDNA flanked with ClaI restriction sites was generated by PCR from a Vamp2-pHluorin plasmid (provided by R.H. Edwards, University of California, San Francisco, San Francisco, CA) and the following oligonucleotide primers: 5′-ATCGATAGCGGCG-GAAGCGG-3′ and 5′-ATCGATTCCGCCGGTTTTGTATAGTTC-ATCC-3′. The ClaI-pHluorin-ClaI cDNA PCR product was then cloned into the modified pcDNA3.1 (+) NCX1.1 plasmid at its new ClaI site to create the final pcDNA3.1-NCX1.1-pHluorin. Stable cells were screened and selected according to the supplier's protocols.

Cell preparation and selection, patch clamp, and Cm recording and imaging

All BHK and T-REx-293 cells were removed from dishes by trypsin and allowed to recover in suspension for 20 min before experiments. In general, relatively large cells were selected for experiments because results were less variable from cell to cell, and our

methods to perfuse pipettes are more facile because larger pipettes can be used with larger cells.

Patch clamp with on-line recording of cell electrical parameters and pipette perfusion was performed as described previously (Yaradanakul et al., 2007; Wang and Hilgemann, 2008). The temperature was 35–37°C, and input resistances were 2–8 MΩ. Unless stated otherwise, square wave voltage perturbation (20 mV; 0.2–1 kHz) was used for Cm measurements. During patch clamp recording without imaging, solution switches were made by rapidly moving the microscope platform by hand so that the cell being monitored was placed directly in front of the solution outlet of interest. The height of solution reservoirs was adjusted to generate flow speeds of at least 2 mm/s in the center of solution streams. Currents that respond immediately to solution changes typically came to >80% of steady state within 100 to 150 ms upon changing solutions. The apparent cell resistances were 0.05–3 GΩ. BHK cells usually had lower resistances than T-REx-293 cells. In our experience, this "resting" resistance reflects mostly the seal–leak pathway in BHK cells. Because the seal resistance pathway does not pass through the entire cell access resistance pathway (Lindau and Neher, 1988), it is impossible to calculate Cm changes accurately when conductance changes may reflect either seal or cell resistance changes. Nevertheless, it can be determined to what extent Cm changes may be misrepresented if exclusively seal or membrane resistance changes are occurring. On this basis, we have discarded all results in which conductance changes potentially affect Cm measurements.

For confocal imaging, a microscope (TE2000-U; 60× oil immersion, 1.45-NA objective; Nikon; RC-26 recording chamber; Warner Instruments) was used with a 40-mW 163-CO_2 laser (Spectra Physics; Newport Corporation) operating at 488 nm and a 1.5 mW Melles Griot cylindrical HeNe laser at 543 nm at 3 and 7% of maximum capacity for pHlourin and FM 4–64 recordings, respectively. Resolution was set to 256 × 256, yielding <1-s exposure times with a pinhole of 100 µm. The bleaching of fluorophores was negligible during experiments.

Solutions and materials

The solutions used minimized all currents other than NCX1 current. Free Mg of all cytoplasmic solutions was 0.4 mM. Standard extracellular solution contained (in mM): 120 LiOH, 4 $MgCl_2$ or 2 $MgCl_2$ plus 2 $CaCl_2$, 20 TEA-OH, 10 HEPES, and 0.5 EGTA, pH 7.0 with aspartate. The standard cytoplasmic solution contained (in mM): 80 LiOH, 20 TEA-OH, 15 HEPES, 40 NaOH, 0.5 $MgCl_2$, 0.5 EGTA, and 0.25 $CaCl_2$, set to pH 7.0 with aspartate. Unless indicated otherwise, 0.2 mM GTP was used in nucleotide-containing solutions. A modified cytoplasmic solution used in myocyte recordings and selected recordings in two companion papers (Editors' Note: This is the first of three companion manuscripts; the other two will appear in the February 2011 issue; Fine et al., 2011; Hilgemann and Fine, 2011) contained (in mM): 60 KOH, 50 NaOH, 15 TEA-OH, 15 HEPES, 0.5 $MgCl_2$, 1.0 EGTA, and 0.2 $CaCl_2$, set to pH 7.0 with aspartate. For pipette perfusion experiments in Fig. 4 (C and D), NaOH was replaced in the cytoplasmic solutions by CsOH. For experiments with spermidine reported in Fig. 8 D, TEA-OH was replaced in standard solutions by 15 LiOH and 5 CsOH, and aspartate was replaced by MES, as removal of all amines except spermidine improved reliability of the protocol. In contrast, the unnatural polyamine, ethylenediamine (EDA), was maximally effective with the standard cytoplasmic solution.

All chemicals were the highest grade available from Sigma-Aldrich, unless indicated otherwise. Recombinant K44A dynamin 2 was provided by J. Albanesi (University of Texas Southwestern Medical Center, Dallas, TX). Commercial *Bacillus cereus* SMase was from Sigma-Aldrich. Because this preparation is not pure, the concentrations used are given as units per milliliter. Purified *Bacillus cereus* SMase was provided by J. Sakurai (Tokushima Bunri University and The University of Tokushima, Tokushima, Japan). Recombinant bacterial SMase was provided by Z. Lu (University of Pennsylvania, Philadelphia, PA).

Preparation of hydroxypropyl-β-cyclodextrin (HPCD)–cholesterol complexes

20 mM HPCD was dissolved in standard extracellular solution, 25% ethanol was added, and the solution was heated under stirring to 70°C. Cholesterol was added slowly while stirring vigorously in 25-µl aliquots from a 40-mM stock solution to give a final concentration of 0.8 mM. The solution was stirred further; heat was applied that induced just-detectable boiling until the volume was reduced to 90% of the original volume without ethanol. Finally, the volume was readjusted with distilled water to the original volume, and the solution was passed through a 0.2-µm filter.

Data analysis and statistics

Experiments were performed in pairwise fashion for each manipulation and its control with each cell batch. Unless indicated otherwise, error bars in the figures give the standard errors for five or more observations, usually seven or more. To simplify figures, "control" results from multiple sets of experiments were pooled when mean results from the different sets were not statistically different. Significance of results was determined by Student's *t* test. Outliers were eliminated using two standard deviations from the mean as criterion. In several figures, a representative experimental record is given together with normalized data points for a dataset. To do so, Cm records were normalized to Cm at a specified time point within each experiment, and then the normalized Cm data points were scaled to Cm at the specified time point in the experiment.

Characteristics of NCX1-mediated Ca transients and Cm changes

Figs. 1 and 2 demonstrate our methods to monitor the electrical properties of cells simultaneously with optical recording of fluorescent probes and manipulation of solutions on both membrane sides. Fig. 1 illustrates the recording of cell capacitance (Cm, measured in picofarads [pF]), membrane currents (I_m), and cellular fluorescence (F) of a Ca indicator by confocal imaging, simultaneously with pipette perfusion to manipulate and/or control the cytoplasmic contents of cells (Yaradanakul et al., 2008). Here, and in most figures, we use BHK cells constitutively expressing cardiac Na/Ca exchangers (NCX1) that can be used to evoke large Ca transients when Ca is applied to the extracellular membrane surface. Patch clamp is established with Ca-free extracellular solution, and cells are positioned in a temperature-controlled solution stream. Then, outward NCX1 current (i.e., Ca influx; see "I_m" record) is activated by applying 2 mM of extracellular Ca for 5 s with high (40 mM) cytoplasmic Na and low (0.5 mM) cytoplasmic EGTA. In this case, a low affinity Ca indicator, Fluo-5N (3 µM; K_d = 90 µM; Takahashi et al., 1999), was included in pipette solutions to allow estimation of free Ca changes. The initial pipette solution contains 0.5 mM EGTA with 0.25 mM Ca (i.e., 0.4 µM of free Ca) and 2 mM ATP. When 2 mM Ca is applied, the current rises rapidly to a peak of 120 pA, decays partially during the application of Ca, and then decays to baseline within 2 s when Ca is being removed. Cm increases by ∼50% during the Ca transient, as vesicles fuse to the cell surface (Yaradanakul et al., 2008). Peak fluorescence occurs at 3 s. Fluorescence begins to decay before the removal of Ca and then decays completely within a few seconds after NCX1 current decays. Upon perfusion of the pipette tip with solution containing 0.5 mM of free Ca (i.e., with 1 mM of total Ca in the 0.5-mM EGTA-containing standard solution), fluorescence rises toward a steady "maximal" level over a time course of ∼1 min. Because the great majority of Ca is bound as Ca enters the cell (Yaradanakul et al., 2008), this time course is

many times longer than the exchange of ions that are not buffered by cell constituents (e.g., potassium). During Ca perfusion, Cm approximately doubles with respect to the pre-perfusion level with a delay to the Ca signal, demonstrating the existence of a large membrane reservoir in these cells. As apparent at the end these records, the increase of Cm during Ca perfusion was followed by a decline. This decline is described in more detail in Fig. 4 (C and D), whereby the decline is larger and occurs more rapidly using highly Ca-buffered pipette solutions. Peak fluorescence during the Ca transient reaches 57% of the maximal fluorescence of dye saturated with 0.5 mM of free Ca. Assuming a K_d of 90 µM for the Fluo3 dye, the peak free Ca occurring during the Ca transient is 157 µM. Thus, these protocols generate Ca transients that exceed normal Ca signaling in cells, except as may occur, for example, during "cell wounding."

Online supplemental material

Complete video recordings of the experiments presented in Fig. 2 (A and B) are provided as part of the online supplemental material. Also, a video record of the myocyte experiment presented in Fig. 11 D is provided. In addition, the following experimental data are provided: Optical measurements of membrane and NCX1 internalization during Ca/polyamine- and SMase-induced MEND (Figs. S1 and S2); control experiments for FM 4–64 and NCX1–pHluorin experiments demonstrating repeatability of protocols without MEND (Fig. S3); experiments demonstrating that MEND results in a loss of inward exchange current (Fig. S4); description of polyamine/Ca-induced MEND in a cell population (Fig. S5); internalization of NCX1 in response to SMase treatment in coverslip-attached cells (Fig. S6); analysis of the ATP dependence of ATP-dependent MEND (Fig. S7); evidence that β-methylcyclodextrin (BMCD)-induced reductions of membrane area (i.e., Cm) result mostly from extraction of cholesterol and phospholipids, rather than endocytosis (Figs. S8 and S9); activation of MEND by multiple SMases, but not by other phospholipases (Fig. S10); experiments demonstrating the long-lived nature of MEND facilitation by Ca (Fig. S11); and description of large capacitance steps often observed during MEND when induced by pipette perfusion of PIP_2 (Fig. S12). The online supplemental material is available at http://www.jgp.org/cgi/content/full/jgp.201010468/DC1.

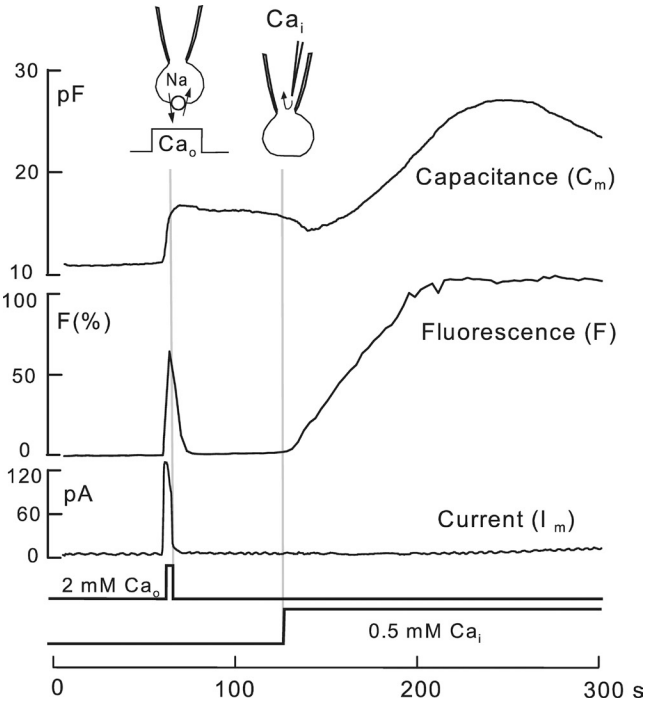

Figure 1. Measurement of Cm and cytoplasmic free Ca changes during the activation of outward NCX1 currents in a BHK cell. The pipette solution contains 0.5 mM EGTA and 0.25 mM Ca (i.e., 0.4 µM of free Ca), 2 mM ATP, no GTP, and 3 µM Fluo 5N (K_d = 90 µM). When 2 mM Ca is applied for 6 s, the current rises to a peak of 120 pA and decays partially during the Ca application. Cm rises by ~50% during this time. Peak fluorescence occurs at 5 s and decays toward baseline with a time constant of ~4 s after deactivation of current. Upon perfusing the pipette tip with 0.5 mM of additional Ca, fluorescence rises to a steady "maximal" level in a nearly linear fashion over 1 min, whereas Cm approximately doubles and then begins to decline, as described in more detail in Fig. 4 (C and D).

RESULTS

Measurement of membrane and NCX1 internalization

To facilitate and abbreviate the subsequent presentation and descriptions of MEND, we describe first our methods to monitor the internalization of membrane per se and of cardiac Na/Ca exchangers using one of the MEND protocols described subsequently. Equivalent data are presented in Figs. S1 and S2 for two other MEND protocols. Full-length videos of the experiments shown in Fig. 2 are available as part of the online supplemental material. In each case, the magnitudes of MEND determined by capacitance recording are verified by optical measurements of FM 4–64 dye uptake into vesicles below the cell surface, and nearly equivalent fractions of Na/Ca exchangers are internalized. In the protocol described in Fig. 2, a large Ca transient is induced by the activation of reverse Na/Ca exchange in the absence of ATP, and MEND is subsequently activated by pipette perfusion of ATP (2 mM) into the cell. Results for the membrane tracer dye, FM 4–64, use BHK cells, and results for NCX1 use the T-REx-293 cell line expressing the pHluorin–NCX1 fusion protein described above.

As illustrated in Fig. 2 A, FM 4–64 binds and unbinds rapidly from BHK cells when applied and removed, thereby defining fluorescence contributed by dye in the outer plasmalemma monolayer. In Fig. S3, we show that, even after prolonged incubation without activating Ca influx, FM 4–64 dissociates nearly completely from BHK cells within seconds. As indicated in Fig. 2 A, the application of Ca for 10 s causes substantial exocytosis. During exocytosis, FM fluorescence increases by 140%, whereas Cm increases by only 59%. Thereafter, fluorescence declines by 73% when dye is washed off, and the presence of a residual fluorescence rim indicates that significant endocytosis occurred during fusion. In all experiments with large exocytic responses, the magnitude of FM fluorescence that washed off within a few seconds was markedly increased, and the reapplication of FM dye then caused a clearly detectable capacitive signal. This capacitive signal is described in more detail in the online

supplemental material of a companion article (Hilgemann and Fine, 2011). Quantitatively, the fluorescence signal corresponding to rapid FM dye binding–unbinding increased on average 30% more than expected from Cm changes during membrane fusion. Thus, FM dye binds more avidly to the cell surface after a large Ca transient.

During MEND in Fig. 2 A, FM fluorescence grows by 15% over 2 min. Thereafter, FM fluorescence decreases by only 35% upon washout of dye, and the response to applying and removing dye is then reduced by 60% compared with the rapid response before MEND. The FM signal that does not wash off amounts to 60% of the rapid response before MEND. Thus, the optical signals are closely consistent with the 65% decline of Cm, reflecting an endocytic response rather than membrane shedding. After the final dye washout, the retained fluorescence (Fig. 2 A, inset) reveals many large vacuoles up to 2.5 µm in diameter. These vacuoles presumably form by the fusion of small vesicles subsequent to their endocytosis, as we do not routinely observe in this protocol capacitance steps that would account for vacuoles being generated in single endocytic steps. We note that the formation of vacuoles during MEND was a variable observation, and that in a majority of cases, the vesicles in the retained fluorescence rim were too small to accurately determine their size optically.

Internalization of NCX1 transporters during MEND is documented in Fig. 2 B using the extracellular NCX1 fusion with the pH-sensitive green fluorescent protein, pHluorin (Miesenböck et al., 1998), which is constitutively expressed in T-REx-293 cells. As evident from the electrical records, Cm responses in T-REx-293 cells were very similar to those of BHK cells. In these experiments, fluorescence corresponding to NCX1 on the cell surface was rapidly determined by switching extracellular solutions from pH 7.0 to 6 to 8. At pH 6, fluorescence of pHluorin is negligible, and the jump on switching from pH 6.0 to 8 defines fluorescence from NCX1 at the cell surface. After one Ca influx episode and perfusion of ATP, Cm declines by >50% from its peak value, and the fluorescence jump from pH 6.0 to 8.0 decreases by 36%. Thus, only ~36% of exchangers are internalized when ~50% of the plasmalemma is internalized. Analysis of inward NCX1 currents, shown in Fig. S4, quantitatively supports the conclusion that NCX1 is not preferentially internalized during MEND. Because fluorescence is increased at pH 6, after Cm has decreased, and fluorescence at pH 8.0 is decreased, NCX1 must enter an intracellular membrane compartment that does not acidify quickly.

In the further presentation of our results, we assume that the Cm changes described reflect the changes of cell surface area as a result of exocytic and endocytic responses with minimal membrane shedding. Besides the optical measurements presented above, which support this interpretation, Figs. S1 and S2 provide similar evidence for two other MEND protocols.

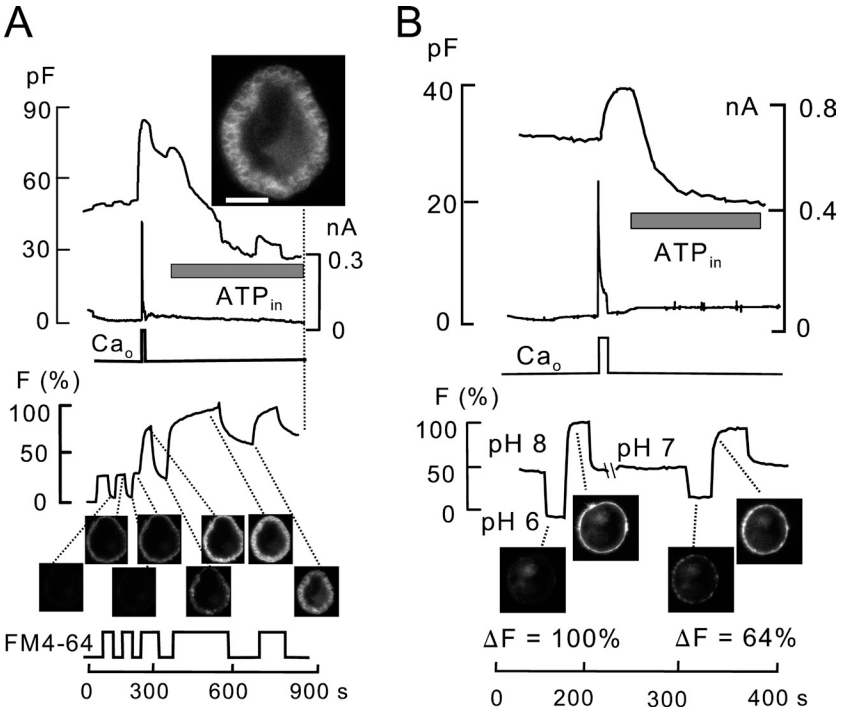

Figure 2. Internalization of membrane and NCX1 exchangers during Ca-promoted MEND with activation by ATP perfusion. (A) Uptake of FM 4–64 dye (8 µM) in a BHK cell subjected to a Ca transient in the absence of ATP followed by cytoplasmic perfusion of 2 mM ATP. As indicated below the Cm record, the cell was maintained in standard solutions without ATP or GTP for 3 min. Outward NCX1 current was activated with 2 mM of extracellular Ca for 10 s, and ~2 min later, 2 mM ATP and 0.2 mM GTP were perfused into the cell. During the experiment, FM dye was applied and removed multiple times to monitor dye binding to the outer cell surface versus dye that had been internalized. After the Ca-activated exocytic response, surface fluorescence is increased 34% more than expected from the increase of Cm. Thereafter, the introduction of nucleotides causes a 65% decrease of Cm, and the "washable" fluorescence decreases by 60% with a corresponding increase of "unwashable" fluorescence. Dye that is trapped in vesicles and vacuoles forms a clear rim close to the cell surface (see inset and Video 1; calibration bar, 10 µm). (B) Internalization of NCX1–pHluorin fusion protein during MEND in a T-REx-293 cell. Using the same ATP perfusion protocol as in A, fluorescence originating from NCX1 at the cell surface was defined by rapid pH jumps from 6 to 8. Subsequent to the decline of Cm by ~45%, the NCX1 fluorescence at the cell surface is decreased by >30%. This internalized pH-insensitive florescence corresponds to the percentage of NCX1 exchangers internalized during MEND, as internalized membrane does not enter acidified compartments.

Two forms of Ca-activated MEND and membrane cycling in BHK cells under control of a polyamine switch

Fig. 3 (A and B) describes two different Ca-activated MEND responses that occur in BHK cells: one that is highly ATP/PIP_2 dependent and one that has no requirement for either ATP or PIP_2. As described in a previous study (Yaradanakul et al., 2008), Ca influx in BHK cells causes exocytic responses that are compensated by approximately equal endocytic responses when cytoplasmic solutions contain 2 mM ATP. As shown in Fig. 3 A, much larger, "excessive" endocytic responses occur when higher, more physiological ATP concentrations are used. With 8 mM ATP, as shown in Fig. 3 A, Cm increases in a few seconds by ~20% during Ca influx and remains stable as long as Ca influx continues. When Ca influx is terminated, Cm remains stable for 10–20 s and then falls over 2 min by nearly 50% from its peak value. As shown in the remainder of the record, these responses can be repeated multiple times with exocytosis and endocytosis amounting to 50% of the cell surface. We note that these exocytic responses decrease only partially with extended exposure to ATP-free solutions (Yaradanakul et al., 2008).

Polyamines (i.e., putrescine, spermidine, and spermine) are ubiquitously present in eukaryotic cells at high concentrations. The free concentration of spermidine, which has gained much recent interest as a promoter of longevity (Kaeberlein, 2009), is in the range of several hundred micromolars (Igarashi and Kashiwagi, 2000). Relevant to this study, polyamines modulate the function of lipid kinases (Coburn et al., 2002), the cytoskeleton (Grant and Oriol-Audit, 1985), and the membrane itself (Schuber et al., 1983). As shown in Fig. 3 B, the presence of 1 mM spermidine in the cytoplasmic solution causes a drastic change of the membrane cycling pattern. Ca influx initially still activates exocytic responses, but exocytosis is rapidly overcome by endocytic responses that decrease Cm by large fractions of total Cm. As illustrated in Fig. 3 B, Cm can recover completely after an endocytic response, and the endocytic responses become larger at subsequent Ca influx episodes. After multiple cycles of endocytosis and exocytosis, one half of cell area is lost in a few seconds during relatively small exchange currents, and Cm recovers over a time course of several minutes. As described later, these endocytic responses do not require ATP, whereas recovery from endocytosis (i.e., exocytosis) is strongly dependent on ATP in cytoplasmic solutions under these conditions. We note that recovery of Cm without ATP was occasionally observed when MEND was initiated <60 s after opening a cell, and when guanosine 5′-[γ-thio]triphosphate (GTPγS) was included in cytoplasmic solutions.

Five different experimental protocols to study Ca-activated MEND

Fig. 4 describes five protocols to induce MEND responses of similar magnitude but different characteristics. Salient features of these responses are noted here, and details are then presented in Figs. 4–7.

1. Ca influx with high cytoplasmic ATP

Fig. 4 A presents the complete electrical parameters of a cell during MEND activated by Ca influx in the presence of high ATP, as in Fig. 3 A. With 8 mM of cytoplasmic ATP, Ca influx by NCX1 for 10 s causes an exocytic response, followed by an "excessive" endocytic response over 1 min with Cm reduced to 50% below baseline. Membrane conductance (G_m) increases transiently during Ca influx, membrane fusion, and the decline of Cm. The increase of G_m during endocytosis occurs with no change of membrane current (I_m) or access resistance (R_a)

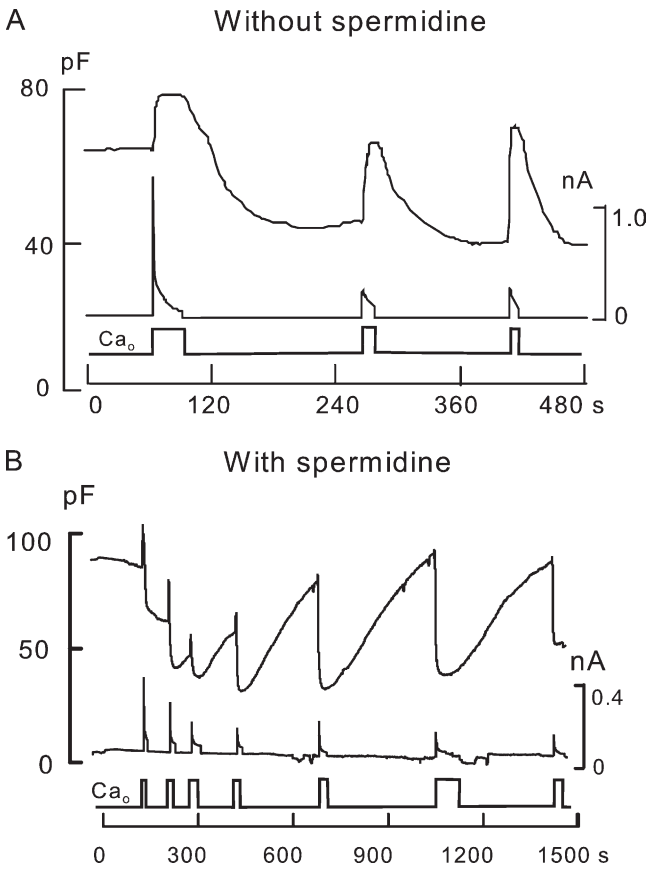

Figure 3. Two types of Ca-activated MEND responses in BHK cells, resulting in membrane recycling by different mechanisms. (A) Using standard cytoplasmic solution with 8 mM ATP and 0.2 mM GTP, the activation of Ca influx by NCX1 for 20 s causes an immediate exocytic response followed by a delayed MEND response that amounts to >50% of the cell surface over 2 min. Cycles of large exocytic responses followed by MEND can then be repeated multiple times in the same cell. (B) Using the same cytoplasmic solution as in A, with an additional 1 mM spermidine, large endocytic responses are initiated during Ca transients, rather than after Ca transients, as in A. Over the course of multiple Ca influx episodes, recovery from MEND becomes more pronounced, and MEND responses amounting to >50% of the cell surface can be repeated multiple times with recovery taking place over several minutes.

and is consistent with the formation of plasmalemma-attached vesicles with low conductance pathways to the extracellular medium, dubbed "fission pores" (Rosenboom and Lindau, 1994). For comparison, a Cm record from a cell without ATP (dotted record) is also shown, similar to >100 recordings. Although exocytic responses are similar to control records (~60% increase of Cm), the decline of Cm is small or absent. As indicated in Fig. 4 A, we estimate that the half-maximal ATP concentration is ~4 mM to support this type of delayed Ca-activated MEND.

2. ATP perfusion after a Ca transient

The second protocol, described in Fig. 4 B, is the same as used in Fig. 2. Experiments are initiated without nucleotides in the cytoplasmic solution. Ca-containing extracellular solution is then applied for 2–4 s to enable reverse Na/Ca exchange, and after a delay of 20 s to 2 min, nucleotides are introduced into the cytoplasm by pipette perfusion. In this example, 2 mM ATP and 0.2 mM GTP were used, and the ensuing MEND amounts to >50% of Cm during the plateau that occurs after Ca influx. Cm begins to recover during this 300-s observation period. Ca transients evoked by reverse exchange current can cause Cm to recover above previous peak values in seconds, reflecting a nearly threefold increase of cell area. An ATP concentration of 0.5 mM was adequate to cause maximal MEND responses in this protocol. However, as described in Fig. S7, the rate of MEND development increases almost linearly with ATP concentration up to 5 mM. Fig. S11 documents that MEND can be initiated several minutes after the Ca transient, indicating that the effect of Ca to promote MEND is long-lived.

3. Pipette perfusion of Ca-buffered solutions

Because Na/Ca exchangers inactivate, cytoplasmic Ca transients caused by reverse exchange current are transient. Therefore, in a third protocol described in Fig. 4 C, Ca-buffered solutions were perfused into cells by pipette perfusion to maintain a high free cytoplasmic Ca concentration. As evident in Fig. 1, high free cytoplasmic Ca can cause an apparent endocytic response over times of 2–3 min. Fig. 4 C shows the more rapid response that occurs when cytoplasmic solutions are heavily buffered to 200 µM of free Ca with nitrilotriacetic acid (NTA; 10 plus 3.5 mM Ca), and the cytoplasmic solution contains 40 mM Cs instead of 40 mM Na. With 0.5 mM ATP, Cm rose on average by 15% within 30 s upon perfusion of Ca and then declined by >40% over 20–80 s. The average fall was 35 ± 3% for eight experiments. Fig. 4 D shows composite results for a series of experiments using five Ca concentrations (n = 4–8 for each group) in the presence of Cs. Fitting the data to a sum of two opposing rectangular hyperbolae, the half-maximal Cm decline occurs at 9 µM of free Ca (Fig. 4 D, solid line). When all data points are fitted to a single hyperbola (Fig. 4 D, gray line), the half-maximum is 26 µM. These characteristics were nearly unchanged when cytoplasmic solutions contained no ATP and a nonhydrolyzable ATP analogue (adenylyl imidodiphosphate [AMP-PNP]; 2 mM), or when they contained no ATP and apyrase (3.5 U/ml) to hydrolyze residual nucleotides. Thus, sustained high cytoplasmic Ca can support a form of MEND that is distinct from ATP-dependent MEND. As described next, polyamines also promote an ATP-independent MEND.

4. Polyamine/Ca-activated MEND

The fourth protocol, described in Fig. 4 E, is to activate Ca influx by NCX1 in the presence of 1 mM of cytoplasmic spermidine, as in Fig. 3 B. In Fig. 4 E, the cytoplasmic solution contains no ATP or GTP, but a profound endocytic response begins within 1–3 s after the initial rise of Cm caused by exocytosis. These MEND responses often exceed 50% of the cell surface in 3 s. We note that MEND responses at a first Ca transient were sometimes small, or even absent, but a second Ca transient usually evoked a rapid MEND. As indicated by a dotted line, MEND responses in this protocol terminated rapidly upon termination of Ca influx and could be reinitiated by reactivating Ca influx. Thus, MEND in this protocol has an immediate requirement for cytoplasmic Ca.

5. Ca influx after plasmalemma enrichment with cholesterol

Clathrin-independent endocytic processes are often inhibited by cholesterol extraction with β-cyclodextrins (Sandvig et al., 2008). As described subsequently, the use of β-cyclodextrins to deplete and enrich membrane cholesterol results in profound inhibition and stimulation of MEND. However, β-cyclodextrins, especially BMCD, can cause substantial decreases of Cm that do not reflect endocytosis (see Figs. S8 and S9). Therefore, we developed another approach to enrich the surface membrane with cholesterol. Using giant excised membrane patches, we previously coated patch pipette tips with inert hydrocarbon mixtures containing lipids of interest and found that some phospholipids incorporated well into the plasmalemma (Hilgemann and Collins, 1992). As a similar approach for cholesterol, we dissolved 100 mg/ml cholesterol in light mineral oil containing 10% ethanol at 60°C. Pipette tips with thick walls (>5 µm at the pipette opening) were then dipped into this mixture before back-filling. The coating did not hinder giga-seal formation or cell opening; it remained adherent during experiments, and recordings without cholesterol (i.e., after coating with the mineral oil/10% ethanol mix) were indistinguishable from recordings with tips without coating.

As shown in Fig. 4 F, using cholesterol-coated pipettes and no spermidine, Ca influx by NCX1 activated MEND

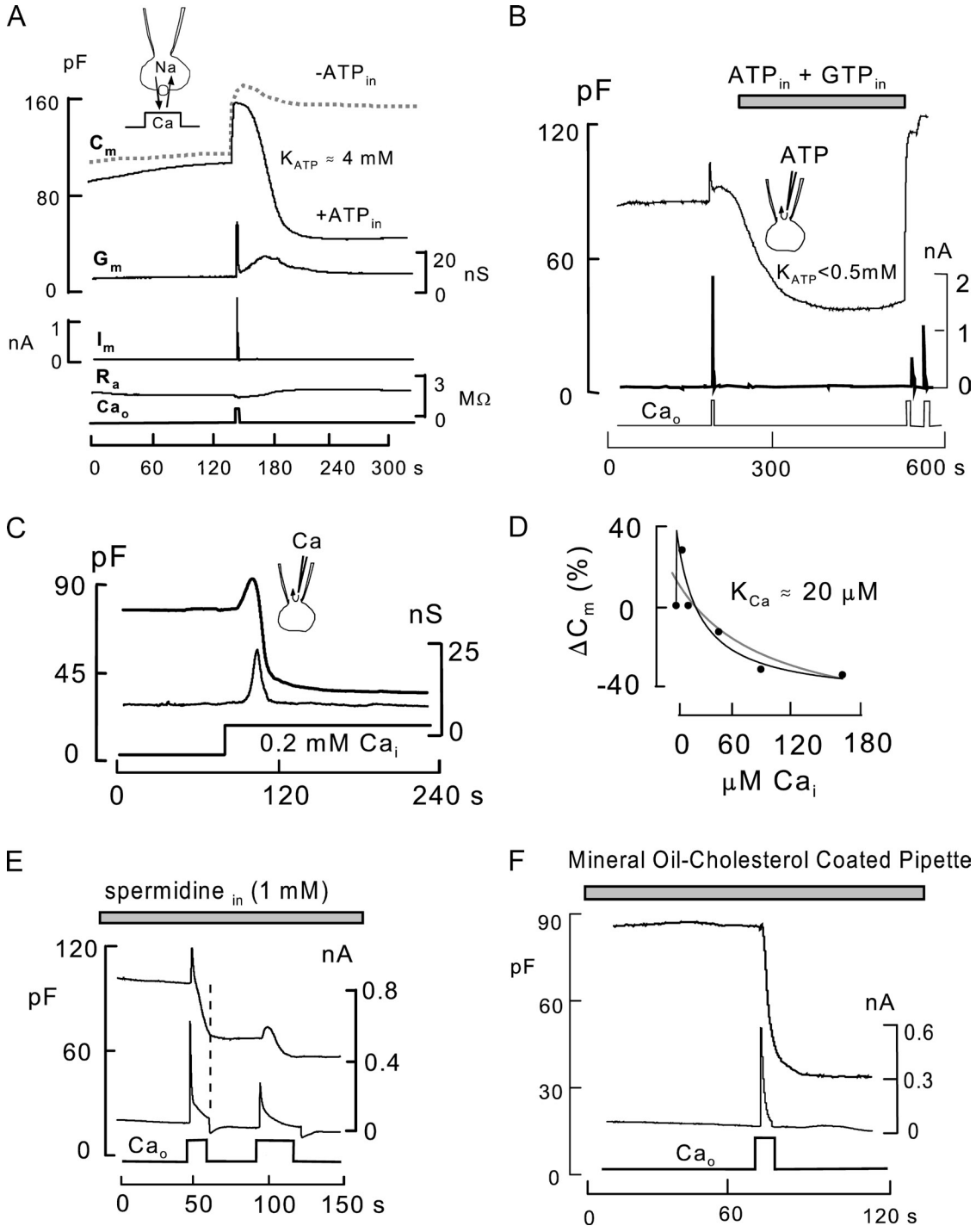

Figure 4. Ca-activated MEND in five different protocols. Electrical parameters are monitored via 0.2–0.5-kHz/20-mV square wave voltage oscillations. (A) MEND with high cytoplasmic ATP (8 mM). From top to bottom, solid records give the calculated cell Cm in pF, conductance (G_m) in nS, membrane current (I_m) in pA, and access resistance (R_a) in MΩ. The dotted record is a representative Cm response of a cell when ATP is omitted from the pipette solution. (B) MEND incurred by perfusion of ATP into cells after nucleotide depletion and the introduction of a Ca transient without nucleotides, as in Fig. 2. The ATP/GTP-free period was 3 min, NCX1 current was activated for 3 s, and 20 s later the pipette was perfused with solution containing 2 mM ATP and 0.2 mM GTP. (C and D) MEND induced by perfusion of Ca-buffered pipette solutions. Cm responses were monitored during pipette perfusion of solutions buffered to free Ca concentrations of 5–200 μM. The experimental record illustrates MEND generated by perfusion of solution with 200 μM of free Ca (10 mM NTA and 0.5 mM ATP plus 0.1 mM GTP). The cytoplasmic solution contains 80 mM Li, 40 mM Cs, and no Na. As shown in the graph for experiments with five different free Ca concentrations, the half-maximal Ca concentration was 9 μM. Standard errors were <15%. (E) Ca-activated MEND in the presence of 1 mM cytoplasmic spermidine. MEND occurs within seconds during Ca influx via NCX1 and stops rather quickly when Ca influx is terminated. (F) Immediate Ca-activated MEND response in a cholesterol-enriched

within a few seconds in the absence of cytoplasmic ATP and spermidine. As evident in the record, endocytic responses were then often so fast that exocytic responses were not evident. On average (>10 observations), MEND in the absence of ATP and polyamines amounted to >50% of the initial Cm of cells.

Detailed studies of Ca-activated MEND subtypes

Figs. 5–8 describe basic properties of the MEND subtypes, and the online supplemental material provides the following additional relevant information: optical measurements of MEND for multiple protocols (Figs. S1 and S2) with control measurements (Fig. S3); documentation that inward Na/Ca exchange currents are down-regulated by ATP-dependent MEND (Fig. S4); an ultrastructural study of MEND using a protocol to induce MEND in cell populations (Fig. S5; in brief, a polyamine that can cross cell membranes [EDA] and enables MEND in response to Ca influx, as verified by uptake of horseradish peroxidase [HRP] into vesicles and vacuoles below the cell surface); demonstration that Na/Ca exchangers are internalized in response to SMase treatment of cells growing on coverslips (Fig. S6); further electrophysiological studies of MEND (Figs. S4, S7, and S10–S12; from several phospholipase types tested, only SMases cause MEND, and PLC activation via overexpressed M1 receptors neither causes nor inhibits Ca/polyamine-dependent MEND); the nucleotide dependence of ATP-dependent MEND; and substantial reductions of Cm induced by BMCD without internalization of Na/Ca exchangers.

Activation of MEND by ATP reflects generation of PIP_2

Fig. 5 presents evidence that ATP promotes MEND via the generation of PIP_2. As shown in Fig. 5 A, ATP-dependent MEND is completely blocked by a high cytoplasmic concentration (0.5 mM) of the nonhydrolyzable GTP analogue, GTPγS. This blockade might reflect the function of many different G proteins, including dynamins. However, as shown in Fig. 5 B, the blockade is fully relieved by including the PLC inhibitor, U73122 (10 µM), in the pipette solution. This reagent, although not specific, powerfully blocks PIP_2 cleavage by PLCs that can be activated by receptor-mediated (Horowitz et al., 2005) and GTPγS-mediated activation of Gq (Camps et al., 1990; Chidiac et al., 1999).

To test whether PIP_2 synthesis indeed underlies the activation of MEND by PIP_2, we first examined the effects of pipette perfusion of PIP_2 into cells in >50 experiments. Under the usual initial conditions of experiments, PIP_2 caused 5–20% declines of Cm (Yaradanakul et al., 2007). Much larger responses were obtained when PIP_2 was perfused into cells after a Ca influx episode with nucleotide-free cytoplasmic solutions. Fig. 5 D shows the composite data for PIP_2 perfusion after one Ca influx episode without ATP. The average Cm decrease was 43 ± 8%. As shown in Fig. 5 C, PIP_2 was also highly effective in the presence of GTPγS (0.5 mM) to block dynamin cycling. In this example, the initial cytoplasmic solution contained, as usual, 0.5 mM EGTA and 0.25 mM Ca. 50 µM PIP_2 was then perfused into the pipette in Ca-free standard solution (3 mM EGTA and no Ca) to block Ca-dependent PLC cleavage of PIP_2. The endocytic response amounts to 65% of peak Cm. An example without GTPγS is provided in Fig. S12.

To determine more directly if PIP_2 plays a role in ATP-activated MEND, we tested whether ATP could be effective in cells perfused with a recombinant phosphoinositol 5-phosphatase, IPP5c (0.1 mg/ml) (Chi et al., 2004). Results are summarized in Fig. 5 E. Using cells that were pre-perfused with cytoplasmic solutions with or without IPP5c, Ca influx by NCX1 was activated for 8 s, and 2 mM ATP was introduced after a delay of 20 s. After ATP, Cm decreased on average 37% in control cells, but only 9% in cells with IPP5c. As described previously (Yaradanakul et al., 2007), peak outward NCX1 currents were nearly unaffected by PIP_2 depletion, although steady-state NCX1 current is PIP_2 sensitive. Collectively, the experiments described in Fig. 5 make a strong case that the generation of PIP_2 is crucial for ATP to induce MEND. Additionally, it is established that both Ca transients and ATP depletion facilitate PIP_2-induced MEND.

Three features of polyamine/Ca-activated MEND

Fig. 6 illustrates three characteristics of polyamine-dependent MEND. The experiments described use nucleotide-free solutions, but these same features were also routinely observed with ATP. As documented both here and in a companion article (Hilgemann and Fine, 2011), MEND can be triggered by many different means after a Ca influx episode. Triggers include perfusion of ATP or PIP_2, cholesterol enrichment, and a second Ca influx episode. However, as shown in Fig. 6 A, polyamines must be present during the Ca transient to promote MEND. Perfusion of 1 mM spermidine into a BHK cell 30 s after inducing a Ca transient, associated with a 40% increase of Cm, causes no MEND (four similar observations).

The second feature highlighted is that Ca-activated MEND can facilitate strongly from one Ca transient to the next. Using 1 mM cytoplasmic spermidine, Fig. 6 B

BHK cell without spermidine. Patch pipettes were dipped in a hot (60°C) mineral oil–cholesterol solution (150 mg cholesterol/1 ml oil with 10% ethanol) before seal formation. Seals were highly stable, and MEND occurred very rapidly upon activating Ca influx, with almost no detectable exocytic response.

shows a common observation that MEND is very small at the first Ca influx episode, whereas a large MEND response occurs at the second and/or third Ca influx episode. Thus, some process set in motion by the first Ca transient enables MEND at a second Ca transient: Ca clearly has long-term and short-term effects. We note also the complete absence of recovery of Cm after MEND in this record without ATP or GTP. Under these conditions, recovery of Cm was invariably negligible when MEND occurred >100 s after opening cells (>50 observations).

The third notable feature of polyamine/Ca-activated MEND, shown in Fig. 6 (C and D), is its insensitivity to high concentrations of GTPγS (0.5 mM), similar to MEND induced by PIP_2 perfusion. In this set of experiments, we used the unnatural polyamine, EDA (2 mM), because occurrence of MEND at the first Ca influx episode was more reliable than with spermidine. Because EDA can cross membranes, we use it on both membrane sides. As shown in Fig. 6 (C and D), the average MEND amounted to 24% of Cm during a single Ca influx episode without GTPγS versus 32% with GTPγS. Thus, neither G protein cycling nor PIP_2 is required for the occurrence of polyamine/Ca-activated MEND.

Cholesterol can activate MEND long after Ca transients subside

As described in Fig. 4 F, a direct method to apply lipids to cells suggests that cholesterol enrichment strongly promotes Ca-activated MEND with no ATP requirement. Fig. 7 extends those results to cholesterol enrichment

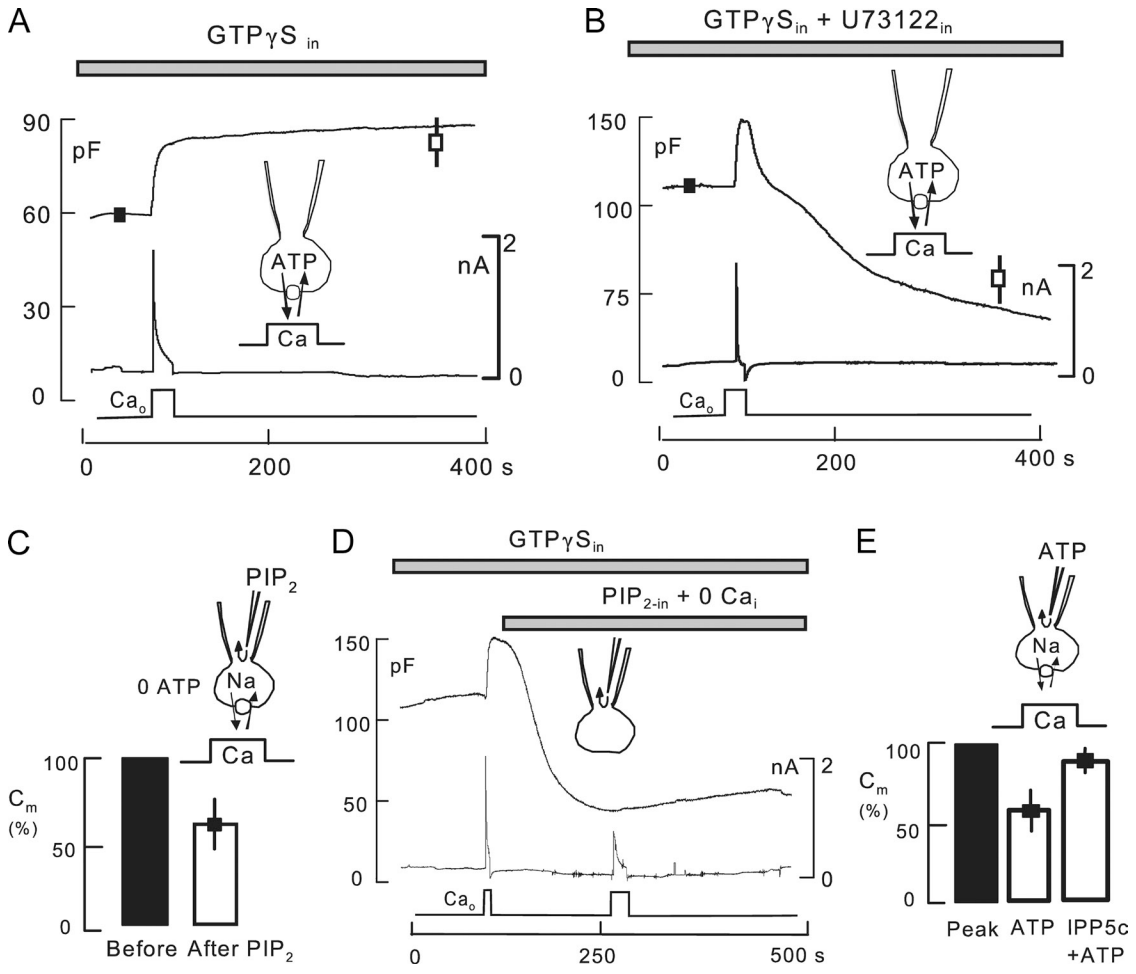

Figure 5. PIP_2 dependence of ATP-activated MEND. PIP_2 mediates ATP-dependent MEND and induces MEND without involvement of G protein cycling. Composite results are expressed as percentage of peak Cm after Ca influx (n = 7–15). (A) Ca-activated MEND with high (8 mM) ATP is blocked by cytoplasmic GTPγS (0.5 mM). (B) Blockade of ATP-dependent MEND by GTPγS, as in A, is relieved by inclusion of the PLC inhibitor, U73122 (10 µM), in the pipette solution. (C) Pipette perfusion of 50 µM PIP_2 substitutes for ATP in the activation of MEND after a Ca transient. Bar graphs give normalized Cm in BHK cells before and after perfusion of 40 µM PIP_2 for 4 min. Before PIP_2 perfusion, cells were perfused with ATP/GTP-free solution for 4 min, followed by NCX1-mediated Ca influx for 6 s. (D) The ability of PIP_2 to induce MEND is unaffected by 0.5 mM GTPγS when PIP_2 is introduced in Ca-free solution (3 mM EGTA). (E) PIP_2 is required for nucleotide reperfusion-induced MEND. Average Cm responses in BHK-NCX1 cells perfused with ATP/GTP-free solution for 4 min, followed by NCX1-mediated Ca influx for 6 s, and then perfusion of 2 mM ATP for 3 min. Inclusion of 0.1 mg/ml IPP5c in cytoplasmic solutions reduced ATP-activated MEND by >80%.

with β-cyclodextrin–cholesterol complexes. To do so, we used HPCD, which extracts phospholipids less potently than the β-methyl form (Ohtani et al., 1989) and therefore is less membrane disruptive. For results in Fig. 7, ATP-, GTP-, and polyamine-free cytoplasmic solutions were used. As shown in Fig. 7 A, exposure of a cell to 10 mM HPCD causes only a small reduction of Cm over 5 min, whereas BMCD often caused decreases of >20% (see also Figs. S8 and S9). After the HPCD treatment, exchange currents and exocytic responses induced by Ca influx are of normal magnitudes for these cells. In contrast to results for free HPCD, Fig. 7 B demonstrates that 10 mM HPCD loaded with 0.8 mM cholesterol causes a small (∼10%) increase of Cm over 5 min (eight similar observations). Thereafter, activation of outward NCX1 current generates large, rapid MEND responses within seconds with almost no exocytic phase. As shown in Fig. 7 C, cholesterol–HPCD complexes evoke large MEND responses (67 ± 9%; $n = 7$) when applied after large Ca transients have primed the membrane for MEND. HPCD complexes themselves caused a smaller, significant decrease (25 ± 5%; $n = 6$), which is described in Fig. S2 of a companion article (Hilgemann and Fine, 2011).

Summary of Ca-activated MEND characteristics

Fig. 8 summarizes extensive experiments suggesting that classical endocytic proteins are not involved in any of the MEND responses described in this paper. In all cases, Cm at the end of the indicated MEND protocol is normalized to peak Cm, whether the peak occurred during or immediately after activation of Ca influx. Group A presents results for Ca-activated MEND in the presence of high (8 mM) ATP, as in Fig. 3 A. MEND was negligible without ATP and amounted on average to only 10% of Cm with 2 mM ATP. A high concentration (5 µM) of the calcineurin inhibitor, FK506, did not alter these responses, whereas BMCD (12 mM for 2 min) effectively blocked the decline of Cm. Fig. 8 B shows composite Cm results for pipette perfusion of solutions with 0.2 mM of free Ca to induce MEND, as in Fig. 4 C, in the presence of 40 mM Cs. MEND was equally large when 2 mM ATP was omitted and cytoplasmic solutions contained 2 mM of nonhydrolyzable ATP (AMP-PNP) or 3.5 U/ml apyrase to hydrolyze residual nucleotides.

Fig. 8 C shows composite Cm results for pipette perfusion of ATP to induce MEND, as in Figs. 2 and 4 B. The average response for perfusion of 2 mM ATP was a 50% decline of Cm. Perfusion of ATP had no effect if the Ca transient was omitted in the protocol. An amphiphysin

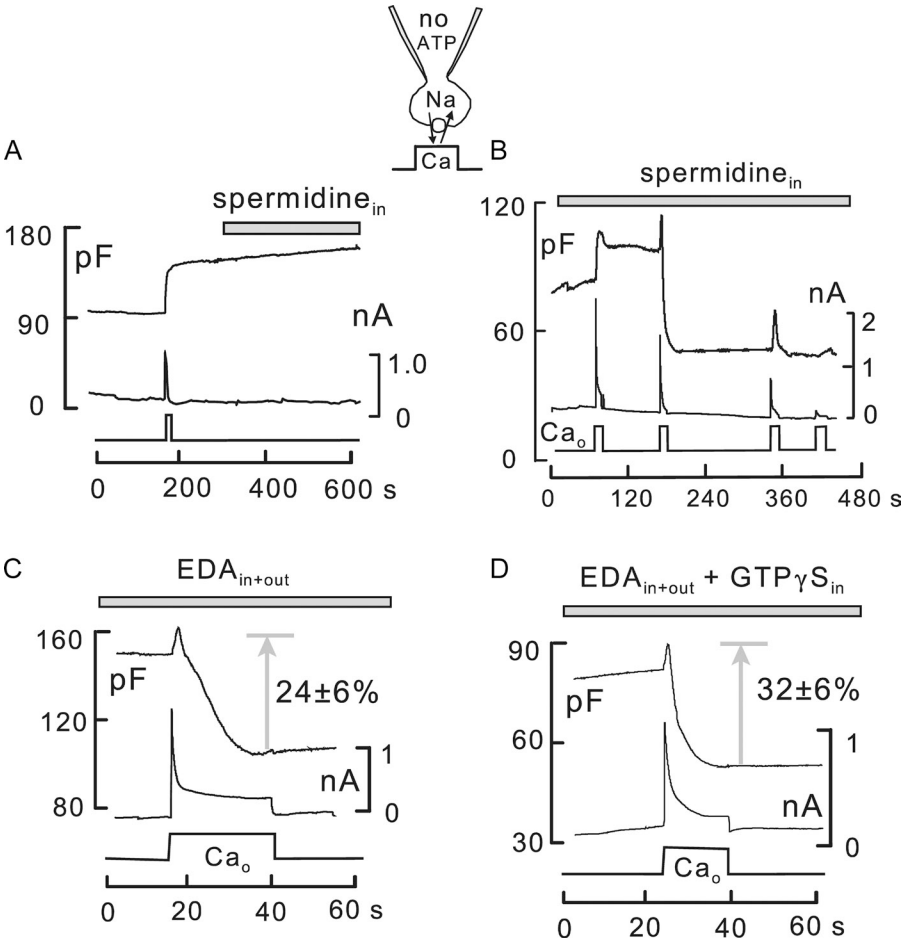

Figure 6. Salient features of polyamine/Ca-activated MEND using nucleotide-free standard cytoplasmic solutions. (A) In contrast to other MEND-promoting agents, spermidine does not cause MEND after a Ca transient has occurred; it must be present in the cytoplasm during the Ca transient. (B) Ca-activated MEND with spermidine is often small at the first Ca influx episode but large and rapid at a second Ca transient. Thus, MEND undergoes long-term facilitation by a mechanism that does not involve phosphorylation. (C) The occurrence of MEND at the first Ca influx episode is more reliable using 2 mM EDA as polyamine in both intracellular and extracellular solutions ($n = 6$). (D) Whereas 0.5 mM GTPγS blocks ATP-dependent MEND (Fig. 5 A), EDA/Ca-activated MEND is unaffected ($n = 7$). Results in C and D are paired experiments from one batch of BHK cells.

sequence, INFFEDNFVPEI (37 μM), which binds AP2 with high affinity (K_d = 2.5 μM) and blocks coat assembly (Gallop et al., 2006), was without effect when included in cytoplasmic solutions. Pipette perfusion of dominant-negative K44A dynamin 2 (0.5 μM) for 5 min did not affect the subsequent response to perfusing ATP. Similar to results with continuous ATP, shown in Fig. 5 A, the nonhydrolyzable GTP analogue, GTPγS (0.2 mM), blocks MEND in this protocol. Deletion of GTP from cytoplasmic solutions can also substantially blunt these MEND responses, perhaps because G proteins such as ARF regulate PIP_2 synthesis (Brown et al., 2001). F-actin disruption with 1 μM latrunculin A in the pipette solution, which results in blatant membrane blebbing, did not block MEND. And finally, the ATP analogue, ATPγS (0.5 mM), did not substitute for ATP in activating MEND, verifying that conventional protein kinases do not mediate the activation of MEND by ATP.

Fig. 8 D shows composite Cm results for Ca-activated MEND in the presence of 1 mM spermidine, as in Fig. 3 B, evaluating MEND after one Ca influx episode of 20-s duration. Omission of ATP and inclusion of 2 mM AMP-PNP did not significantly change the MEND response. As described above, 2 mM EDA can substitute for spermidine to promote MEND, whereas pentalysine (Lys5) cannot. The inclusion of 0.5 mM GTPγS resulted in a partial inhibition of the MEND response to one Ca transient, as verified by two sets of experiments with seven and eight observations in the presence of GTPγS. For three reasons, we conclude that GTPγS specifically

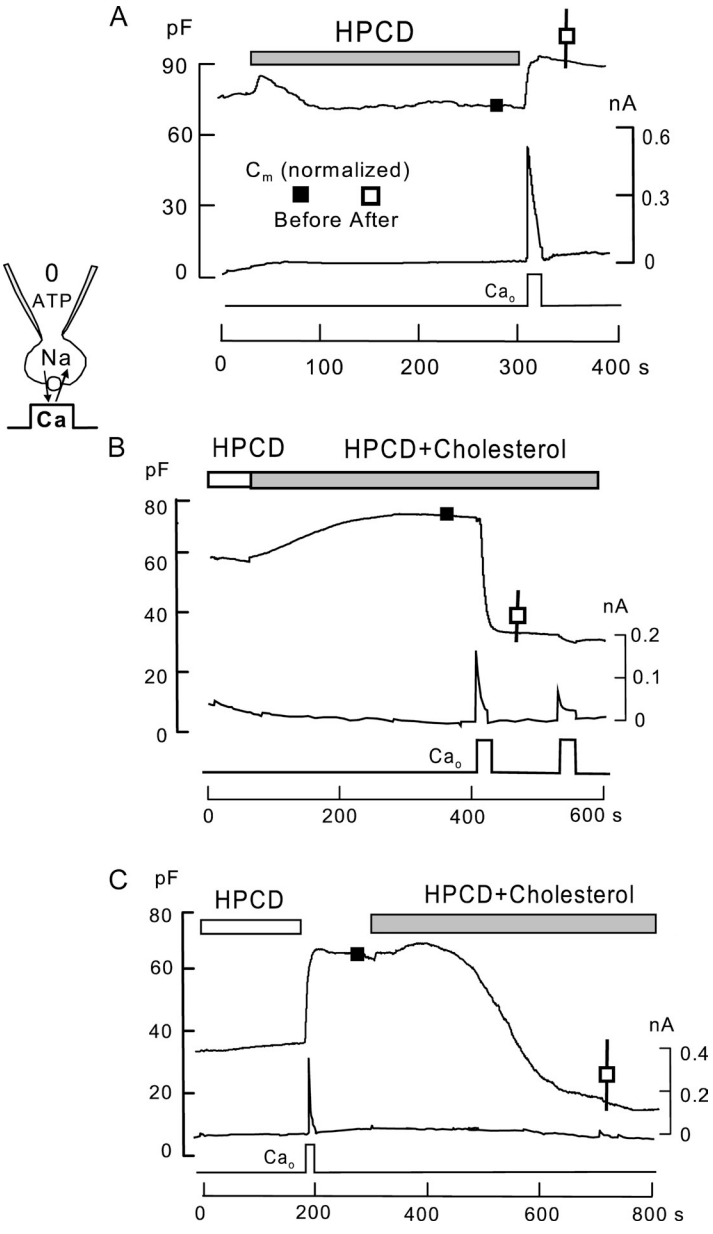

Figure 7. Cholesterol enrichment enables fast Ca-activated MEND without polyamines. All results use BHK cells with ATP-, GTP-, and polyamine-free cytoplasmic solution. Composite Cm changes from multiple experiments (n = 4–6) are plotted by normalizing Cm after an intervention (open squares with standard errors) to Cm values before the intervention (filled squares). (A) Treatment of BHK cells with 10 mM HPCD for 5 min does not affect in an evident manner NCX1 currents or membrane fusion responses evoked by outward NCX1 current. Cm decreases by <10% during HPCD treatment. (B) Treatment of BHK cells with cholesterol-loaded HPCD for 5 min causes an average increase of Cm of 12%. Thereafter, the activation of outward NCX1 current causes an average 36% fall of Cm within 5 s, often with no evident preceding membrane fusion response. (C) Calcium transients force cells into a MEND-permissive state for many minutes. Although treatment of cells with HPCD complexes does not cause endocytic responses in control cells (see B), cholesterol enrichment causes profound MEND over 2–4 min when treatment is initialized after an NCX1-mediated Ca transient.

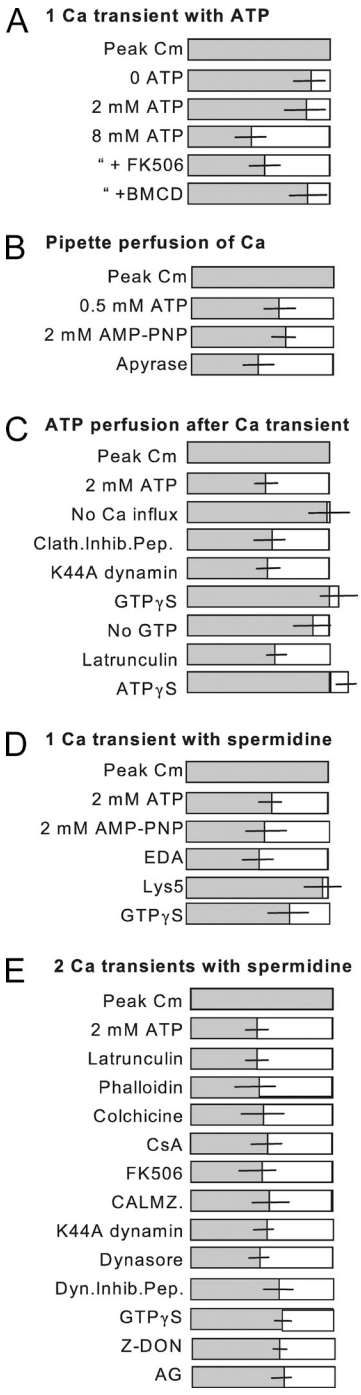

Figure 8. Composite results of experiments characterizing MEND in five protocols. Bar graphs represent the peak Cm occurring in an experiment, during or shortly after a Ca transient, in relation to Cm after the occurrence of MEND. Each dataset reflects five or more observations. (A) MEND occurring with the indicated cytoplasmic ATP concentrations in response to a single Ca influx episode of 12–16 s. (B) MEND occurring upon pipette perfusion of an NTA-buffered solution with 0.2 mM of free Ca. (C) MEND occurring upon pipette perfusion of 2 mM ATP and 0.2 mM GTP after the cells were opened and maintained without nucleotides for 3 min and exposed to one Ca influx episode for 2 s. (D) MEND occurring during a single Ca influx episode for 15 s in the presence of cytoplasmic spermidine (1 mM). (E) MEND occurring over two Ca influx episodes of 15-s duration, separated by 2 min, in the presence of cytoplasmic spermidine (1 mM). See Results for complete details.

increases the variability of MEND occurrence with spermidine at a first Ca transient, noted in connection with Fig. 6 B. First, GTPγS does not blunt MEND in the presence of EDA (Fig. 6 D). Second, individual MEND responses in the presence of GTPγS amounted to >60% of the cell surface. And third, as described next, MEND responses at a second Ca transient brought Cm closer to the "control" MEND values.

Fig. 8 E describes further experiments using two Ca influx episodes of 15 s separated by 2 min to induce MEND. All agents tested were added to pipette solutions. Cytoskeleton modifiers (3 μM latrunculin A, 10 μM phalloidin, and 30 μM colchicine) were without a significant effect, as were cyclosporin (CsA; 5 μM); FK506 (10 μM); calmidazolium (CALMZ; 12 μM); overexpression of dominant-negative K44A dynamin 2 with GFP to identify transfected cells; the dynamin inhibitor, dynasore (200 μM) (Newton et al., 2006); and an unmyristolated dynamin inhibitor peptide (50 μM; DynPep; Tocris Bioscience). As noted above, MEND was less affected by GTPγS (0.5 mM) using two Ca influx episodes than with one episode. We tested for a role of Ca-activated transglutaminases because polyaminylation was suggested earlier to play a role in endocytosis (Davies et al., 1980). Inhibitors of transglutaminases (e.g., dansylcadaverine [Davies et al., 1980] and Z-DON-Val-Pro-Leu-OMe; Zedira) and amino oxidases (1 mM; aminoguanidine [AG]) (Brunton et al., 1991) had small inhibitory effects, equivalent to GTPγS.

We turn now to the membrane itself. As noted in the Introduction, a role for SMases and ceramide generated by SMases appeared attractive, because exocytic events might bring both SMases and ceramide into the extracellular membrane surface. Figs. 9–11 document the potential of SMases to generate MEND as well as arguments against a major role for SMases and ceramide in Ca-activated MEND.

MEND induced by extracellular SMases

Fig. 9 describes MEND induced within seconds in BHK cells by the extracellular application of SMase from *Bacillus cereus*. Results in Fig. 9 (A and C) are with the commercial preparation (1 U/ml; Sigma-Aldrich), and results in B are with a purified enzyme (Ago et al., 2006). Although the commercial preparation contains additional enzymatic activities (Ramu et al., 2007), results for the two preparations were indistinguishable. Further, we demonstrate in Fig. S10 that recombinant bacterial SMase from *Bacillus anthrax* is similarly effective to induce MEND.

Bacillus cereus SMase requires Ca (or manganese) to adsorb to the surface of cells (Tomita et al., 1983).

Therefore, solutions with 0.5 mM of free extracellular Ca (0.5 mM EGTA with 1.0 mM of added Ca) were used. When using cells that expressed cardiac NCX1, we used Na-free, Li-based cytosolic solutions to avoid Ca influx. Fig. 9 A shows records of cell electrical parameters determined by square wave voltage perturbation. In this experiment, the cytoplasmic solution contained no ATP or GTP to mimic ATP-depleted conditions of the previous cellular study (Zha et al., 1998). As shown first, the application and removal of 2 mM Ca have no effect under these Na-free conditions. Upon applying SMase, together with Ca, Cm (46 pF) begins to decrease within a few seconds, achieves a maximal rate of decline of >12% per second, and stabilizes at about one half of the initial value. A small, transient rise of cell conductance mirrors the rate of change of Cm (dC_m/dt), whereas membrane current (I_m) and access resistance (R_a) do not change.

Because sphingomyelin is present mostly in the outer plasmalemma monolayer, we tested whether SMase has any effect from the cytoplasmic side. Representative for five similar experiments, Fig. 9 B shows that perfusion of purified SMase (5 µg/ml) into the cytoplasm of BHK cells in the presence of 5 µM of free Ca (5 mM EGTA with 4.5 mM Ca) caused at most a 12% decrease of Cm over 4 min, whereas the application of the same enzyme concentration to the outside causes a MEND response amounting to 65% of the cell surface in a few seconds.

Fig. 9 C shows one Cm record of SMase-induced MEND with high ATP and GTP concentrations (8 and 0.2 mM, respectively) and one without nucleotides, whereby Cm is normalized to its value at the start of the experiments. Composite results for four and five observations, respectively, are given as data points with error bars. In the presence of ATP, Cm recovered for the most part over several minutes after MEND, whereas there was no recovery in the absence of ATP. Membrane internalized with SMase treatment was found previously to recycle back to the cell surface by following transferrin receptor trafficking (Zha et al., 1998). Using the optical approaches described in Materials and methods, Fig. S2 shows that SMase-induced MEND internalizes membrane and Na/Ca exchangers in equivalent fractional amounts.

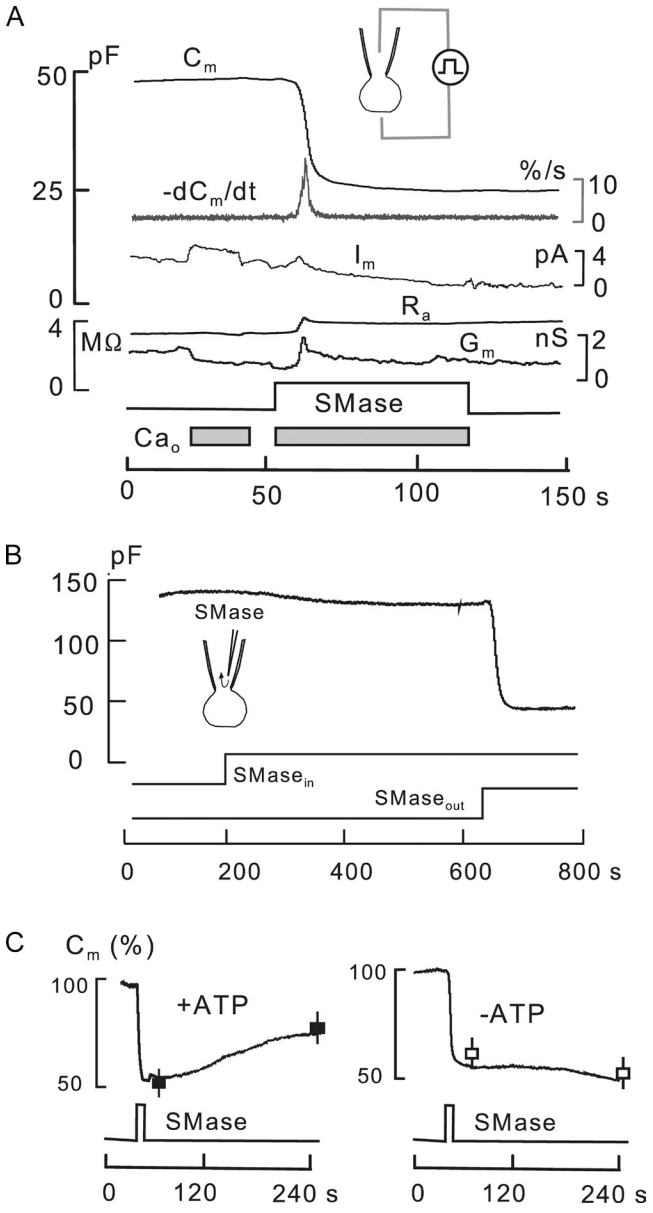

Figure 9. Activation of MEND by the extracellular application of 1 U/ml *Bacillus cereus* SMase in BHK fibroblasts with Na-free solutions. (A) BHK cell perfused for >2 min with Na-, ATP-, and GTP-free cytoplasmic solution. The application of 1 mM Ca from outside has no effect on Cm, whereas the application of Ca with SMase causes a 54% drop of Cm at a peak rate of 12% per second. Membrane current (I_m) shows no response, access resistance (R_a) increases by 10%, and membrane conductance increases transiently by 0.8 nS in parallel with the first derivative of Cm ($-dC_m/dt$). (B) Cytoplasmic application of SMases does not cause MEND. Perfusion of purified SMase into the cytoplasm of a BHK cell causes at most 12% decline of Cm at the same concentration that causes >50% decline of Cm from outside within seconds. (C) Reversal of SMase-induced MEND. SMase application as in A caused on average a 53% fall of Cm within 15 s. With 6 mM ATP in the cytoplasmic solution (left), Cm recovered toward baseline by 60% over 5 min, whereas Cm did not recover in the absence of nucleotides (right).

Failure to confirm a role for secreted acid SMase in Ca-activated MEND

In the recent article by Tam et al. (2010), a role for acid SMases in Ca-activated endocytosis was supported by multiple experimental approaches. We describe here equivalent experiments with BHK cells using chemical probes that provided arguments for SMase involvement in endocytosis. Our results for both probes are inconsistent with the involvement of secreted SMases in MEND.

Desipramine treatments do not block MEND

The amphipathic drug, desipramine, is considered to be a powerful reagent to displace acid SMases from

membranes and over time to promote its degradation (Tam et al., 2010). In the study of Tam et al., cells were treated with 50 µM desipramine for 1 h. Thereafter, endocytosis in response to cell wounding appears to be blocked because FM dye uptake in the protocol used is blocked. Using equivalent desipramine treatments, we do not find significant inhibition of MEND responses in our protocols. To ensure that desipramine treatment was adequate, we incubated BHK cells with 100 µM desipramine for 1 h before removing them from dishes, and thereafter we incubated cells again for 1 h at 37°C with 100 µM desipramine in the absence of serum. In some experiments, we also added 100 µM desipramine to both cytoplasmic and extracellular solutions to promote the loss of SMase activities. As described in Fig. 10 A, MEND responses to Ca influx in the presence of high ATP (8 mM, as in Fig. 3 A) were entirely normal, amounting to >50% of the cell surface on average (n = 7). As shown in Fig. 10 B, MEND responses to Ca influx in the presence of 1 mM spermidine (i.e., as in Fig. 3 B) were entirely normal, amounting to loss of ∼50% of the cell surface on average (n = 7) within a few seconds.

MEND and Ca-activated exocytosis can occur independently

A second argument of Tam et al. (2010) for a role of secreted SMase in endocytic responses, subsequent to cell wounding, is that endocytosis was blocked when exocytosis was blocked, thereby establishing a causal relationship. As a means to block exocytosis, cells were treated with a high concentration (50 µM) of the alkylating "active site" reagent, bromoenol lactone (BEL), which was suggested to block exocytosis. As described in Fig. 10 C, we find that the equivalent BEL treatments of BHK cells indeed fully block endocytic responses, subsequent to Ca influx. However, we find that exocytic responses continue robustly with multiple Ca influx cycles, resulting in a doubling of membrane area in response to multiple Ca transients. We note that the conditions of experiments presented in Fig. 10 C are otherwise identical to

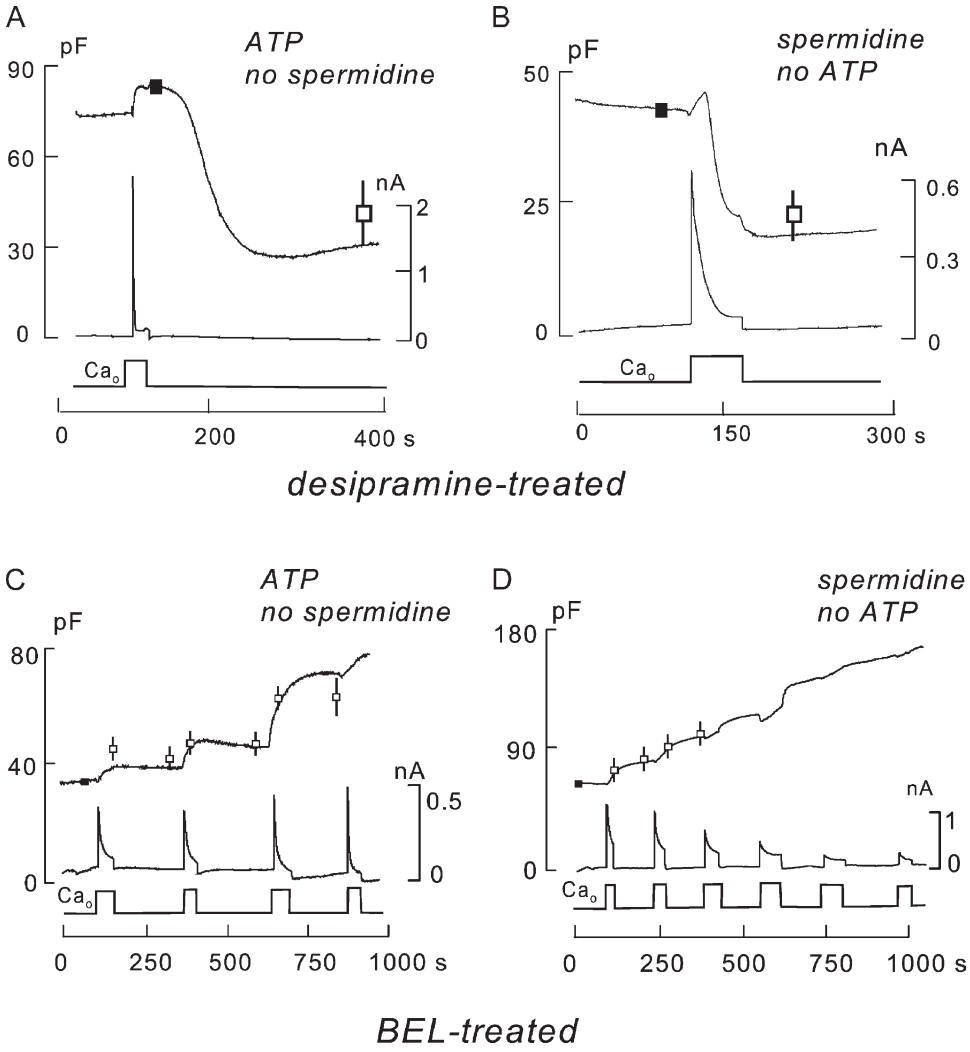

Figure 10. Desipramine treatment does not block MEND, whereas BEL treatment blocks MEND but not exocytosis. (A) ATP-dependent MEND in response to a Ca transient is unchanged by the pretreatment of cells with 100 µM desipramine for 1 h in serum-free media, followed by further incubation with 100 µM desipramine for 1 h and execution of experiments with 100 µM desipramine in both cytoplasmic and extracellular solutions. (B) Similar treatment with desipramine fails to inhibit spermidine-dependent MEND in the absence of ATP. (C) Same solutions as in A. BHK-NCX1 cells, which were pretreated with 50 µM BEL for 1 h in serum-free media, show robust Ca-activated exocytosis, with Cm doubling over three Ca influx episodes while endocytic responses are potently inhibited. (D) Same solutions as in B, with BEL treatment as in C. BEL treatment does not block exocytic responses that occur in the absence of ATP and presence of cytoplasmic spermidine (1 mM). However, endocytic responses are completely suppressed.

those used in Fig. 10 A (i.e., with 8 mM of cytoplasmic ATP). Similarly, as described in Fig. 10 D, we find that exocytic responses continue robustly in the equivalent protocols with 1 mM of cytoplasmic spermidine and no ATP. Over several cycles of Ca influx, exocytosis results in a full doubling membrane area, whereas endocytosis is entirely blocked. Thus, the reagents used by Tam et al. (2010) provide no evidence in our hands for the hypothesis that acid SMase might be involved in Ca-activated MEND responses.

MEND occurs in cardiac myocytes without exocytosis and can be initiated by spontaneous Ca release

Also relevant to the conclusions of Tam et al. (2010) is that MEND occurs in cardiac myocytes without preceding exocytosis, as we describe in Fig. 11. Because BHK and HEK293 cells are highly proliferative and do not exhibit global Ca transients, we tested for the existence of MEND in adult mouse and rat cardiac myocytes, using native NCX1 to generate Ca influx and to initiate cycles of spontaneous Ca release. Indeed, outward NCX1 currents (0.2–0.5-nA peaks) caused large declines of Cm in both mouse and rat myocytes. Experiments described in Fig. 11 use the modified standard solution, described in Materials and methods, with 6 mM ATP and no polyamines. Fig. 11 A shows an example from a rat myocyte. Activation of reverse exchange current for just 2 s initiates a reversible endocytic response. Cm declines rapidly during Ca influx and then more slowly as spontaneous contractile activity initiated by Ca influx declines. We stress the time course of MEND in relation to the second and third Ca influx episodes: MEND clearly continues after Ca influx is terminated, suggesting that internal Ca release can drive MEND. Typical for all myocytes studied, Cm recovers progressively more slowly after each MEND response.

Because myocytes contract vigorously in this protocol, we tested the possibility that contraction might cause

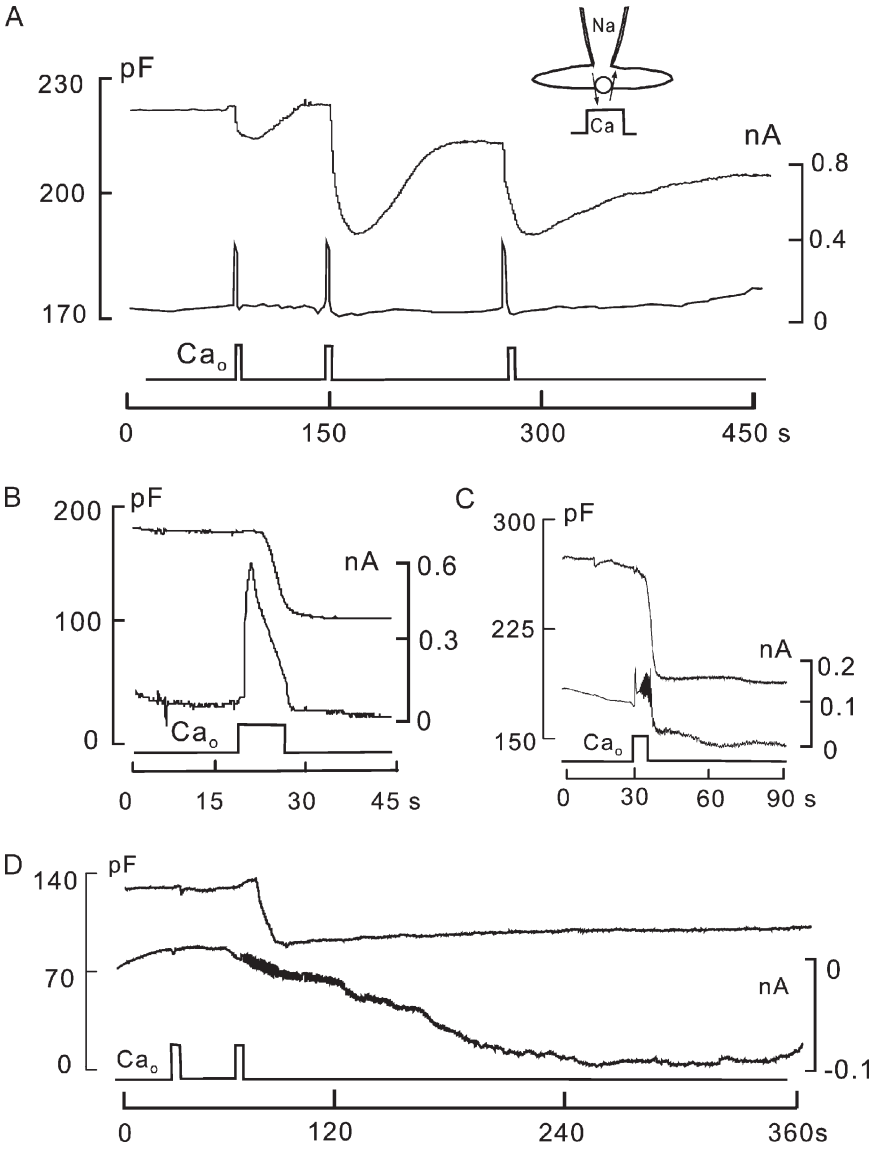

Figure 11. MEND occurs in cardiac myocytes without preceding exocytic responses and can be induced by spontaneous cycles of Ca release. (A) Rat cardiac myocyte with 6 mM of cytoplasmic ATP. MEND develops rapidly during activation of NCX1 and continues for several seconds after terminating Ca influx as cells continued to contract spontaneously. MEND reversal in myocytes is labile, becoming substantially slower from one MEND cycle to the next. Reversal was negligible when MEND was allowed to proceed to a final loss of >30% of the cell surface. (B–D) Different patterns of MEND responses observed in mouse cardiac myocytes. (B) Mouse myocyte with contraction blocked by 17 µM blebbistatin. Na/Ca exchange current is relatively large. MEND begins within 3 s of activating Ca influx, and MEND terminates when exchange current is deactivated. (C) Mouse myocyte without blebbistatin. Brief activation of reverse exchange current promotes spontaneous cycles of Ca release, accompanied by transient current changes that are evident in the current record. MEND begins with no exocytic response and terminates spontaneously as spontaneous contractile activity terminates. (D) Mouse myocyte without blebbistatin. Exchange current is negligibly small. The application of Ca activates spontaneous cycles of Ca release accompanied by transient current changes. MEND begins after extracellular Ca has been removed and during spontaneous contractile activity, and it terminates spontaneously with no evident relationship to the termination of spontaneous activity. The bright field record of this experiment is provided as Video 3.

T-tubules to be physically pinched off by contractile activity. To do so, we used high concentrations of the myosin 2 inhibitor, blebbistatin (17 µM), in both cytoplasmic and extracellular solutions to block contraction (Farman et al., 2008). In >20 observations, MEND remained robust when contraction was abolished in both rat and mouse myocytes. As shown in Fig. 11 B for a mouse myocyte, activation of exchange current for 10 s resulted in Cm declines of >25% after a 2–3-s delay with no preceding exocytic response. Thus, it is unlikely that MEND is caused by contractile activity or by the exocytosis of ceramide/SMase-rich membrane.

Depending on myocyte batch and time after isolation, exchange currents can be very small or negligible in mouse myocytes. Fig. 11 (C and D) illustrates that in such myocytes, the application of extracellular Ca initiated cycles of spontaneous Ca release and contraction that were accompanied by MEND, which occurred after termination of Ca influx. Spontaneous activity in these myocytes can be followed electrophysiologically via transient current changes that occur synchronously with contraction. In Fig. 11 C, spontaneous activity occurs during the application of Ca and terminates synchronously with MEND after Ca influx is deactivated. In Fig. 11 D, Ca was applied twice for just 3 s. On the first Ca application, a single cycle of Ca release was evoked. The second application of Ca, however, caused a prolonged train of Ca release cycles. MEND both begins and terminates after the removal of extracellular Ca, demonstrating that MEND can be initiated by internal Ca release in myocytes. A bright field optical record of this experiment, provided as Video 3, documents that MEND is occurring with modest contractile activity that does not cause prolonged myocyte shortening.

DISCUSSION

Large Ca transients promote large endocytic responses in BHK cells enriched in ATP, polyamines, or cholesterol. As summarized in cartoon form in Fig. 12, the underlying mechanisms appear to be "non-canonical." Ca acts via multiple calmodulin-independent mechanisms, whereas ATP acts via generation of PIP_2 without classical adapters or dynamins. Membrane recycling can occur in two different ways. Ca influx can cause ATP-independent membrane fusion followed by ATP-dependent endocytosis (Fig. 3 A), or Ca influx can cause ATP-independent endocytosis followed by ATP-dependent vesicle recycling to the cell surface (Fig. 3 B). Thus, these protocols should facilitate analysis of multiple partial reactions of membrane recycling. We discuss first the relevance of Ca-activated MEND described here to previous work and then the mechanisms by which Ca promotes MEND, bringing results from companion articles (Fine et al., 2011; Hilgemann and Fine, 2011) to bear on this study. Finally, we discuss how Ca-activated MEND may be promoted by PIP_2, polyamines, and cholesterol.

The physiological relevance of Ca-activated MEND

Ca transients used to trigger MEND in this study usually exceed 100 µM of free Ca (Fig. 1). Thus, the results are clearly relevant to cell wounds that flood cells with Ca (Idone et al., 2008). As noted in the Introduction, such wounds are closed by fusion of internal membranes to the cell surface, followed by endocytosis of plasmalemma into compartments that do not acidify (Cocucci et al., 2004). Besides having relatively high Ca requirements, similar to cell wound–induced endocytosis, the vesicles formed during MEND also do not readily acidify upon internalization (Figs. 2 B and S1 B).

The relevance of Ca-activated MEND to other physiological endocytic mechanisms studied previously is less secure. MEND can clearly be triggered by smaller Ca transients when multiple Ca transients occur (e.g., Fig. 3 B). In myocytes, MEND can be induced by cycles of spontaneous Ca release initiated by "trigger" amounts of Ca influx (Fig. 11 A). Thus, it is established that physiological Ca signals can initiate MEND. When cytoplasmic free Ca is clamped by Ca buffers, MEND develops over

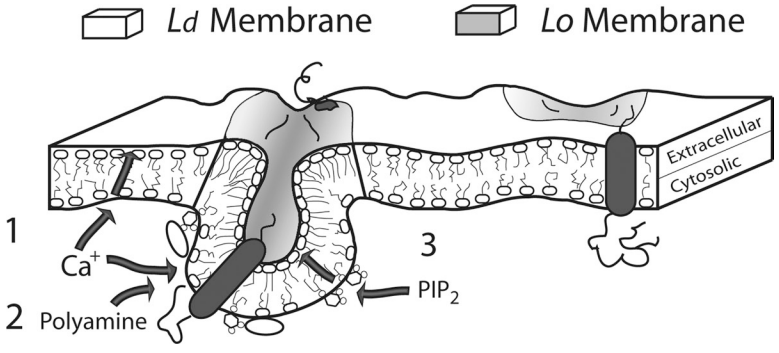

Figure 12. Ca-activated endocytosis involves three distinct processes. (1) Large Ca transients cause long-term changes of the outer plasmalemma monolayer that promote endocytosis (Hilgemann and Fine, 2011). Possible mechanisms include the generation of lipids that promote the growth of lipid domains (i.e., the coalescence of small domains to large domains) and/or the translocation of such lipids to the outer monolayer. (2) In synergy with spermidine, high cytoplasmic Ca causes inner monolayer changes that promote endocytosis. One possible mechanism is the coalescence of lipid domains by Ca- and lipid-binding proteins (e.g., annexins) (Chasserot-Golaz et al., 2005). (3) After membrane modification by Ca, the ATP-dependent synthesis of PIP_2 promotes MEND by Ca-independent mechanisms. The clustering of PIP_2 and PIP_2-binding proteins may promote transbilayer domain coupling and membrane buckling that in turn drives endocytosis.

the free Ca range of 10 to 35 µM (Fig. 4 D). With the exception of skeletal muscle, this represents a range that may occur locally at Ca influx and release sites, but not globally (Clapham, 2007). "Excessive endocytosis" in secretory cells (Thomas et al., 1994; Smith and Neher, 1997; Engisch and Nowycky, 1998) and "bulk endocytosis" in synapses (Clayton et al., 2009) are both clathrin independent, consistent with a mechanistic relationship to Ca-activated MEND described here. However, dynamin 1 is implicated to trigger and/or drive bulk endocytosis (Clayton et al., 2009), whereas dynamins appear to play no role in MEND. Recent knockout studies in mice show that dynamin 1 (Ferguson et al., 2007) and AP2 (Kim and Ryan, 2009) are in fact not required for basal neuronal function (i.e., membrane cycling). Possibly therefore, mechanisms related to MEND maintain basal membrane recycling in those animal models. In this context, MEND might represent a core endocytic mechanism that becomes exploited, modified, and/or regulated by dynamins and other classical endocytic proteins.

Recently, fast Ca-activated, clathrin/dynamin-independent endocytosis has been described in astrocytes (Jiang and Chen, 2009), reminiscent of Ca-activated MEND. In skeletal muscle, intense activity promotes the reversible formation of vacuoles from transverse tubules (Lännergren et al., 2002), and the MEND responses described here in cardiac myocytes (Fig. 11) may be related. Ca-activated MEND could play many roles in cardiac myocytes. In pathological circumstances, the removal of Na/Ca exchangers from the plasma membrane would protect from Ca overload (Shen et al., 2007).

Toward a mechanistic understanding of MEND

Our initial goal was to determine which classical endocytic proteins control and/or drive Ca-activated MEND. However, no positive outcomes emerged. We first addressed clathrin; to our knowledge, it has never been questioned that clathrin-dependent endocytic processes require cytoplasmic potassium, and our experiments all use potassium-free solutions. Second, in the case of ATP-dependent MEND, a clathrin-binding domain of amphiphysin at a high concentration had no disrupting effect (Fig. 8 C). Third, the formation and fission of large vesicles (Fig. S12) are not consistent with clathrin involvement, and rapid formation of vacuoles (Fig. 2 A) seems questionable for clathrin-dependent endocytosis. In protocols that induce MEND under ATP-free conditions, PIP_2 will be depleted by lipid phosphatases (Hilgemann, 2007; Falkenburger et al., 2010). If not immediately depleted, Ca transients will rapidly deplete PIP_2 by PLC activation (Yaradanakul et al., 2007). However, MEND still occurs, often at a second or third Ca transient (e.g., Fig. 6 B), as well as in the presence of a high GTPγS concentration (Figs. 5, B and D, and 6 D). Thus, polyamine-dependent MEND clearly does not require PIP_2 and might even be inhibited by PIP_2. Therewith, a role for adapters and G proteins that use PH domains is eliminated.

In no protocol did dynamin inhibitory peptides or dominant-negative dynamins effectively block MEND (Fig. 8). Dynamin cycling requires GTP hydrolysis (Song et al., 2004). However, GTPγS at high concentrations does not block ATP-dependent MEND when PLCs are simultaneously inhibited and thereby PIP_2 hydrolysis is blocked (Fig. 5 B). GTPγS does not block PIP_2-activated MEND in the presence of Ca chelators (Fig. 5 D), and it does not block polyamine-dependent MEND effectively (Figs. 6 D and 8, D and E). Furthermore, reagents that inhibit calmodulin-dependent processes and disrupt actin cytoskeleton had no clear effect on MEND (Fig. 8). In summary, we have uncovered no evidence that Ca-activated MEND in BHK and HEK293 cells involves adapters, dynamins, or actin cytoskeleton.

The mechanisms of Ca action in MEND

Ca-activated MEND is strongly dependent on physical properties of the membrane itself. It is blocked by brief β-cyclodextrin treatments (Fig. 8 A). It is drastically promoted by cholesterol enrichment by either a direct method (Fig. 4 F) or by cholesterol–HPCD complexes (Fig. 7). Exocytosis is then overwhelmed by MEND with >50% of the cell surface internalized within a few seconds.

Several observations suggest that exocytosis is not a prerequisite for the occurrence of MEND. First, MEND responses in the presence of spermidine or after cholesterol enrichment are extremely fast and large, and they can occur with almost no preceding exocytic phase. Second, spermidine-dependent MEND facilitates from one Ca transient to the next, so that exocytic responses nearly exhaust the supply of vesicles before MEND occurs. Third, fast Ca-activated MEND occurs in ventricular cardiac myocytes that do not display Ca-activated exocytic responses (Fig. 11).

Ca appears to act by both long-term and immediate mechanisms. Regarding the long-term effect, our central observation is that large Ca transients facilitate subsequent MEND responses for several minutes after Ca transients subside. Triggers for a subsequent MEND response include a rise of cytoplasmic PIP_2 (Fig. 5, C and D), a second Ca transient (Fig. 6 B), membrane enrichment with cholesterol (Fig. 7 C), and the extracellular application of certain detergents (Hilgemann and Fine, 2011). Given that rather low concentrations of nonionic detergents cause MEND that is similar to Ca-activated MEND (Fine et al., 2011), the long-term effect of Ca may be the generation of MEND-promoting lipids. Ca-binding proteins of an unknown identity, dubbed "scramblases," facilitate movement of lipids between monolayers in all eukaryotic cells when free Ca rises into the range of tens of micromolars (Bevers and Williamson, 2010). Thus, the immediate effect of Ca could be to promote the translocation of

a MEND-promoting lipid from the cytoplasmic to the extracellular monolayer, independent of membrane fusion–derived lipids.

An alternative hypothesis arises from the fact that Ca-activated MEND internalizes primarily membrane with a high content of liquid-ordered (*Lo*) membrane (Hilgemann and Fine, 2011). According to one theoretical model, nano- to microscopic membrane buckling can cause the coalescence of extracellular *Lo* domains into buds (Minami and Yamada, 2007). In this context, Ca might act primarily through transmembrane or membrane-binding proteins that upon binding Ca induce the formation of membrane "caps" and "valleys," followed by domain coalescence, budding, and vesiculation.

Failure to implicate ceramide or phospholipases in Ca-activated MEND

Phospholipases provide a plethora of mechanisms that might generate MEND-promoting lipids. We find up to now that PLCs and PLA_2s do not promote endocytic responses, whereas extracellularly applied bacterial SMases are very effective (Figs. 9, S2, and S10), consistent with a previous report for ATP-depleted fibroblasts (Zha et al., 1998). The generation of ceramide is relevant because large Ca transients (Babiychuk et al., 2008) and metabolic stress (Pavoine and Pecker, 2009) can both promote sphingomyelin breakdown. In giant liposomes, ceramide generated by SMases coalesces into domains that rapidly vesiculate to the opposite membrane side (Bollinger et al., 2005). Thus, accumulation of ceramide during ATP depletion (Fig. 3) and over multiple Ca-transient cycles (Figs. 9 and 10) might facilitate MEND.

Nevertheless, using the same interventions that Tam et al. (2010) used with positive outcomes, we find no support for SMase and/or ceramide involvement in Ca-activated MEND. In this regard, it is not certain that the assays used by Tam et al. monitor the same exocytic and endocytic responses occurring in our experiments. Ca-activated exocytosis is not blocked by tetanus toxin light chain in the cells used by us (Wang and Hilgemann, 2008), although tetanus toxins block membrane resealing after cell wounding in 3T3 cells (Togo et al., 1999) and in sea urchin eggs and embryos (Bi et al., 1995). On the one hand, exocytosis in our experiments may be mechanistically different from exocytosis during cell wound responses. On the other hand, different sensitivities to tetanus toxins may reflect differences in the SNAREs expressed in different cell types (Wang and Hilgemann, 2008). Neither ATP-dependent nor polyamine-dependent MEND is suppressed by prolonged exposure to high concentrations of desipramine and/or its acute application on both membrane sides (Fig. 10), suggested to suppress acid SMase activities (Tam et al., 2010). The reagent used by Tam et al. to block exocytosis, BEL, does not do so in our protocols (Fig. 10, C and D). Rather, it powerfully blocks endocytosis while allowing Ca-activated exocytosis to occur unabated. Unusually, exocytosis continues for prolonged periods after Ca influx is terminated (Fig. 10, C and D). This may reflect an unbridling of the exocytic mechanism, but alternatively a very effective blockade of endocytosis may reveal "hidden," opposing exocytic events. Clearly, the hypothesis of Tam et al. now requires support by other lines of evidence that Niemann-Pick type A mutations cause defects in endocytic pathways.

The blockade of both ATP- and polyamine-promoted MEND by BEL opens a new pathway to elucidate the molecular basis of Ca-activated MEND. The $iPLA_2$s that BEL inhibits most potently act as either mixed or selective PLA1/PLA_2s (Yan et al., 2005; Cedars et al., 2009), whereby the generation of 2-arachidonoyl lysophosphatidylcholine and its metabolites would be inhibited. From a companion study (Fine et al., 2011), it is known that lysophospholipids can induce MEND, similar to detergents. A caveat is that exogenous lysolipids dissociate rapidly from cell membranes, whereas the action of Ca to promote MEND is long-lived. We stress for now, therefore, that BEL may well be acting nonspecifically at the concentrations used here, and that cysteines, serines, and amines can all potentially be covalently modified.

The mechanisms by which PIP_2, polyamines, and cholesterol promote MEND

Given that classical endocytic proteins and actin cytoskeleton are not involved in MEND and that MEND internalizes selectively ordered membrane domains (Fine et al., 2011; Hilgemann and Fine, 2011), PIP_2, polyamines, and cholesterol enrichment must all act in pathways that lead to domain coalescence, budding, and fission.

PIP_2 synthesis is coupled to the organization of most endocytic processes described to date (Doherty and McMahon, 2009), and PIP_2 must be cleaved or dephosphorylated for fission to proceed in multiple cases, including actin-dependent endocytosis in yeast (Stefan et al., 2002) and phagocytosis in macrophages (Botelho et al., 2000). It has long been suggested that "lipid rafts," which are enriched in sphingomyelin and cholesterol on the extracellular side, are enriched in PIP_2 on the cytoplasmic side (Liu et al., 1998). Although the biophysical basis for coupling across monolayers remains enigmatic, our data forces us to suggest that PIP_2 on the cytoplasmic side organizes the membrane for endocytosis by promoting the coalescence of membrane domains on the extracellular side. We can neither support nor contradict an involvement of membrane proteins at this time: PIP_2 might promote the association of PIP_2-binding proteins into complexes or promote conformational changes of membrane proteins that cause domain coalescence via membrane buckling. In either case, it will be of great interest to determine whether PIP_2 must be

dephosphorylated before fission proceeds in delayed PIP_2-dependent MEND.

From the extracellular side, it is described in a companion article (Fine et al., 2011) that certain amphipathic compounds (e.g., dodecylsulfate) promote a reorganization of membrane domains that predisposes them to internalize while blocking the final fission event until they are washed away. By a similar principle, PIP_2 on the cytoplasmic side might promote membrane reorganization that supports endocytosis but still hinder the final fission events, a hindrance that might be overcome by local activity of either phosphatases or dynamins. In this connection, we note that "excessive" endocytosis in chromaffin cells may be inhibited by PIP_2 because it is enhanced by overexpression of the inositol 5-phosphatase domain of synaptojanin 1 (Milosevic, I., personal communication). Polyamine/Ca-activated MEND may be similar because multiple Ca transients in ATP-depleted cells, which progressively deplete PIP_2 (Yaradanakul et al., 2007), cause progressively larger Ca/polyamine-activated MEND responses (Fig. 6 B).

Spermidine overcomes the requirement for PIP_2 in Ca-activated MEND. Up to now, we have only been able to negate prominent candidate mechanisms in this effect (Fig. 8 D). These include actin bundling, Ca-activated transglutaminases, and amino oxidases. Direct effects of Ca and polyamines on the membrane require further attention. Polyamines might promote anionic lipids, especially phosphatidylserine, to form domains that substitute for PIP_2-containing domains in promoting MEND. Both old and new studies provide a reminder that the Ca-binding sites that activate MEND can potentially be anionic phospholipids: Micromolar polyamine concentrations greatly reduce Ca requirements for aggregation and fusion of vesicles containing acidic phospholipids and cholesterol (Schuber et al., 1983). In membranes containing zwitterionic lipids, PIP_2, and cholesterol, Ca at concentrations of 2–10 μM can cause the formation of PIP_2-rich domains (Levental et al., 2009). From many possible protein effectors, Ca/lipid-binding annexins are clearly attractive candidates, as individual annexins have been shown to promote the formation of membrane domains (Chasserot-Golaz et al., 2005).

Cholesterol may facilitate both domain coalescence and membrane bending (Groves, 2007; Sarasij et al., 2007). The remarkable dependence of Ca-activated MEND on the membrane cholesterol content (Figs. 4 F and 7) underscores that endocytosis may potentially regulate the cholesterol content of the membrane. In this connection, we note the probable explanation for one confusing experimental result related to cholesterol studies: Cyclodextrins used to extract cholesterol can cause substantial declines of membrane capacitance primarily by extracting membrane constituents, rather than by promoting endocytosis (see Figs. S10 and S11).

In summary, Ca promotes MEND by two mechanisms that do not appear to require clathrin, dynamins, or F-actin turnover. ATP promotes MEND by supporting the synthesis of PIP_2. Ca promotes polyamine-dependent MEND by one mechanism that requires the immediate presence of Ca and another mechanism that accumulates over multiple Ca transients, separated by many seconds and even minutes. Calmodulin does not appear to be involved in either of these actions. Cholesterol content of the membrane is a strong determinant of the occurrence and extent of Ca-activated MEND.

We thank Jun Sakurai (Tokushima Bunri University and The University of Tokushima, Tokushima, Japan) for purified *B. cereus* neutral SMase; James H. Hurley (National Institutes of Health, Bethesda, MD) for recombinant IPP5c; Zhe Lu (University of Pennsylvania, Philadelphia, PA) for recombinant anthrax SMase; Sherry Sours-Brothers, Annamaria Assunta Nasti, Chengcheng Shen, and Jeremy Leitz (University of Texas Southwestern Medical Center, Dallas, TX) for expert assistance and discussion; Harvey McMahon (Medical Research Council, Cambridge, England, UK) for the amphyphysin-based peptide; Joseph Albanesi (University of Texas Southwestern Medical Center, Dallas, TX) for dynamins, dynamin constructs, and discussion; and Kenneth Philipson and Debora Nicoll (University of California, Los Angeles, Los Angeles, CA) for advice, discussion, and NCX1 constructs.

This work was supported by RO1-HL067942 and HL513223 to D.W. Hilgemann.

Edward N. Pugh Jr. served as editor.

Submitted: 3 May 2010
Accepted: 6 December 2010

REFERENCES

Ago, H., M. Oda, M. Takahashi, H. Tsuge, S. Ochi, N. Katunuma, M. Miyano, and J. Sakurai. 2006. Structural basis of the sphingomyelin phosphodiesterase activity in neutral sphingomyelinase from Bacillus cereus. *J. Biol. Chem.* 281:16157–16167. doi:10.1074/jbc.M601089200

Altankov, G., and F. Grinnell. 1995. Fibronectin receptor internalization and AP-2 complex reorganization in potassium-depleted fibroblasts. *Exp. Cell Res.* 216:299–309. doi:10.1006/excr.1995.1038

Artalejo, C.R., A. Elhamdani, and H.C. Palfrey. 1996. Calmodulin is the divalent cation receptor for rapid endocytosis, but not exocytosis, in adrenal chromaffin cells. *Neuron.* 16:195–205. doi:10.1016/S0896-6273(00)80036-7

Babiychuk, E.B., K. Monastyrskaya, and A. Draeger. 2008. Fluorescent annexin A1 reveals dynamics of ceramide platforms in living cells. *Traffic.* 9:1757–1775. doi:10.1111/j.1600-0854.2008.00800.x

Bevers, E.M., and P.L. Williamson. 2010. Phospholipid scramblase: an update. *FEBS Lett.* 584:2724–2730. doi:10.1016/j.febslet.2010.03.020

Bi, G.Q., J.M. Alderton, and R.A. Steinhardt. 1995. Calcium-regulated exocytosis is required for cell membrane resealing. *J. Cell Biol.* 131:1747–1758. doi:10.1083/jcb.131.6.1747

Bollinger, C.R., V. Teichgräber, and E. Gulbins. 2005. Ceramide-enriched membrane domains. *Biochim. Biophys. Acta.* 1746:284–294. doi:10.1016/j.bbamcr.2005.09.001

Botelho, R.J., M. Teruel, R. Dierckman, R. Anderson, A. Wells, J.D. York, T. Meyer, and S. Grinstein. 2000. Localized biphasic changes in phosphatidylinositol-4,5-bisphosphate at sites of phagocytosis. *J. Cell Biol.* 151:1353–1368. doi:10.1083/jcb.151.7.1353

Brown, F.D., A.L. Rozelle, H.L. Yin, T. Balla, and J.G. Donaldson. 2001. Phosphatidylinositol 4,5-bisphosphate and Arf6-regulated

membrane traffic. *J. Cell Biol.* 154:1007–1017. doi:10.1083/jcb.200103107

Brunton, V.G., M.H. Grant, and H.M. Wallace. 1991. Mechanisms of spermine toxicity in baby-hamster kidney (BHK) cells. The role of amine oxidases and oxidative stress. *Biochem. J.* 280:193–198.

Camps, M., C.F. Hou, K.H. Jakobs, and P. Gierschik. 1990. Guanosine 5′-[gamma-thio]triphosphate-stimulated hydrolysis of phosphatidylinositol 4,5-bisphosphate in HL-60 granulocytes. Evidence that the guanine nucleotide acts by relieving phospholipase C from an inhibitory constraint. *Biochem. J.* 271:743–748.

Cedars, A., C.M. Jenkins, D.J. Mancuso, and R.W. Gross. 2009. Calcium-independent phospholipases in the heart: mediators of cellular signaling, bioenergetics, and ischemia-induced electrophysiologic dysfunction. *J. Cardiovasc. Pharmacol.* 53:277–289.

Chan, S.A., and C. Smith. 2001. Physiological stimuli evoke two forms of endocytosis in bovine chromaffin cells. *J. Physiol.* 537:871–885. doi:10.1113/jphysiol.2001.012838

Chasserot-Golaz, S., N. Vitale, E. Umbrecht-Jenck, D. Knight, V. Gerke, and M.F. Bader. 2005. Annexin 2 promotes the formation of lipid microdomains required for calcium-regulated exocytosis of dense-core vesicles. *Mol. Biol. Cell.* 16:1108–1119. doi:10.1091/mbc.E04-07-0627

Chi, Y., B. Zhou, W.Q. Wang, S.K. Chung, Y.U. Kwon, Y.H. Ahn, Y.T. Chang, Y. Tsujishita, J.H. Hurley, and Z.Y. Zhang. 2004. Comparative mechanistic and substrate specificity study of inositol polyphosphate 5-phosphatase Schizosaccharomyces pombe Synaptojanin and SHIP2. *J. Biol. Chem.* 279:44987–44995. doi:10.1074/jbc.M406416200

Chidiac, P., V.S. Markin, and E.M. Ross. 1999. Kinetic control of guanine nucleotide binding to soluble Galpha(q). *Biochem. Pharmacol.* 58:39–48. doi:10.1016/S0006-2952(99)00080-5

Clapham, D.E. 2007. Calcium signaling. *Cell.* 131:1047–1058. doi:10.1016/j.cell.2007.11.028

Clayton, E.L., and M.A. Cousin. 2009. The molecular physiology of activity-dependent bulk endocytosis of synaptic vesicles. *J. Neurochem.* 111:901–914. doi:10.1111/j.1471-4159.2009.06384.x

Clayton, E.L., V. Anggono, K.J. Smillie, N. Chau, P.J. Robinson, and M.A. Cousin. 2009. The phospho-dependent dynamin-syndapin interaction triggers activity-dependent bulk endocytosis of synaptic vesicles. *J. Neurosci.* 29:7706–7717. doi:10.1523/JNEUROSCI.1976-09.2009

Coburn, R.F., D.H. Jones, C.P. Morgan, C.B. Baron, and S. Cockcroft. 2002. Spermine increases phosphatidylinositol 4,5-bisphosphate content in permeabilized and nonpermeabilized HL60 cells. *Biochim. Biophys. Acta.* 1584:20–30.

Cocucci, E., G. Racchetti, P. Podini, M. Rupnik, and J. Meldolesi. 2004. Enlargeosome, an exocytic vesicle resistant to nonionic detergents, undergoes endocytosis via a nonacidic route. *Mol. Biol. Cell.* 15:5356–5368. doi:10.1091/mbc.E04-07-0577

Davies, P.J., D.R. Davies, A. Levitzki, F.R. Maxfield, P. Milhaud, M.C. Willingham, and I.H. Pastan. 1980. Transglutaminase is essential in receptor-mediated endocytosis of alpha 2-macroglobulin and polypeptide hormones. *Nature.* 283:162–167. doi:10.1038/283162a0

de Haro, L., G. Ferracci, S. Opi, C. Iborra, S. Quetglas, R. Miquelis, C. Lévêque, and M. Seagar. 2004. Ca2+/calmodulin transfers the membrane-proximal lipid-binding domain of the v-SNARE synaptobrevin from cis to trans bilayers. *Proc. Natl. Acad. Sci. USA.* 101:1578–1583. doi:10.1073/pnas.0303274101

Doherty, G.J., and H.T. McMahon. 2009. Mechanisms of endocytosis. *Annu. Rev. Biochem* 78:857–902.

Engisch, K.L., and M.C. Nowycky. 1998. Compensatory and excess retrieval: two types of endocytosis following single step depolarizations in bovine adrenal chromaffin cells. *J. Physiol.* 506:591–608. doi:10.1111/j.1469-7793.1998.591bv.x

Falkenburger, B.H., J.B. Jensen, and B. Hille. 2010. Kinetics of PIP_2 metabolism and KCNQ2/3 channel regulation studied with a voltage-sensitive phosphatase in living cells. *J. Gen. Physiol.* 135:99–114. doi:10.1085/jgp.200910345

Farman, G.P., K. Tachampa, R. Mateja, O. Cazorla, A. Lacampagne, and P.P. de Tombe. 2008. Blebbistatin: use as inhibitor of muscle contraction. *Pflugers Arch.* 455:995–1005. doi:10.1007/s00424-007-0375-3

Ferguson, S.M., G. Brasnjo, M. Hayashi, M. Wölfel, C. Collesi, S. Giovedi, A. Raimondi, L.W. Gong, P. Ariel, S. Paradise, et al. 2007. A selective activity-dependent requirement for dynamin 1 in synaptic vesicle endocytosis. *Science.* 316:570–574. doi:10.1126/science.1140621

Fine, M., M.C. Llaguno, V. Lariccia, M.-J. Lin, A. Yaradanakul, and D.W. Hilgemann. 2011. Massive endocytosis driven by lipidic forces originating in the outer plasmalemmal monolayer: a new approach to membrane recycling and lipid domains. *J. Gen. Physiol.* In press.

Gallop, J.L., C.C. Jao, H.M. Kent, P.J. Butler, P.R. Evans, R. Langen, and H.T. McMahon. 2006. Mechanism of endophilin N-BAR domain-mediated membrane curvature. *EMBO J.* 25:2898–2910. doi:10.1038/sj.emboj.7601174

Goñi, F.M., and A. Alonso. 2009. Effects of ceramide and other simple sphingolipids on membrane lateral structure. *Biochim. Biophys. Acta.* 1788:169–177. doi:10.1016/j.bbamem.2008.09.002

Grant, N.J., and C. Oriol-Audit. 1985. Influence of the polyamine spermine on the organization of cortical filaments in isolated cortices of Xenopus laevis eggs. *Eur. J. Cell Biol.* 36:239–246.

Groves, J.T. 2007. Bending mechanics and molecular organization in biological membranes. *Annu. Rev. Phys. Chem.* 58:697–717. doi:10.1146/annurev.physchem.56.092503.141216

Hilgemann, D.W. 2007. Local PIP(2) signals: when, where, and how? *Pflugers Arch.* 455:55–67. doi:10.1007/s00424-007-0280-9

Hilgemann, D.W., and A. Collins. 1992. Mechanism of cardiac Na(+)-Ca2+ exchange current stimulation by MgATP: possible involvement of aminophospholipid translocase. *J. Physiol.* 454:59–82.

Hilgemann, D.W., and M. Fine. 2011. Mechanistic analysis of massive endocytosis in relation to functionally defined surface membrane domains. *J. Gen. Physiol.* In press.

Holopainen, J.M., M.I. Angelova, and P.K. Kinnunen. 2000. Vectorial budding of vesicles by asymmetrical enzymatic formation of ceramide in giant liposomes. *Biophys. J.* 78:830–838. doi:10.1016/S0006-3495(00)76640-9

Horowitz, L.F., W. Hirdes, B.C. Suh, D.W. Hilgemann, K. Mackie, and B. Hille. 2005. Phospholipase C in living cells: activation, inhibition, Ca^{2+} requirement, and regulation of M current. *J. Gen. Physiol.* 126:243–262. doi:10.1085/jgp.200509309

Hryshko, L.V., D.A. Nicoll, J.N. Weiss, and K.D. Philipson. 1993. Biosynthesis and initial processing of the cardiac sarcolemmal Na(+)-Ca2+ exchanger. *Biochim. Biophys. Acta.* 1151:35–42. doi:10.1016/0005-2736(93)90068-B

Idone, V., C. Tam, J.W. Goss, D. Toomre, M. Pypaert, and N.W. Andrews. 2008. Repair of injured plasma membrane by rapid Ca2+-dependent endocytosis. *J. Cell Biol.* 180:905–914. doi:10.1083/jcb.200708010

Igarashi, K., and K. Kashiwagi. 2000. Polyamines: mysterious modulators of cellular functions. *Biochem. Biophys. Res. Commun.* 271:559–564. doi:10.1006/bbrc.2000.2601

Ivanov, A.I. 2008. Pharmacological inhibition of endocytic pathways: is it specific enough to be useful? *Methods Mol. Biol.* 440:15–33. doi:10.1007/978-1-59745-178-9_2

Jiang, M., and G. Chen. 2009. Ca2+ regulation of dynamin-independent endocytosis in cortical astrocytes. *J. Neurosci.* 29:8063–8074. doi:10.1523/JNEUROSCI.6139-08.2009

Kaeberlein, M. 2009. Spermidine surprise for a long life. *Nat. Cell Biol.* 11:1277–1278. doi:10.1038/ncb1109-1277

Katz, B. 1996. Neural transmitter release: from quantal secretion to exocytosis and beyond. The Fenn Lecture. *J. Neurocytol.* 25:677–686. doi:10.1007/BF02284834

Kim, S.H., and T.A. Ryan. 2009. Synaptic vesicle recycling at CNS snapses without AP-2. *J. Neurosci.* 29:3865–3874. doi:10.1523/JNEUROSCI.5639-08.2009

Lännergren, J., H. Westerblad, and J.D. Bruton. 2002. Dynamic vacuolation in skeletal muscle fibres after fatigue. *Cell Biol. Int.* 26:911–920. doi:10.1006/cbir.2002.0941

Levental, I., D.A. Christian, Y.H. Wang, J.J. Madara, D.E. Discher, and P.A. Janmey. 2009. Calcium-dependent lateral organization in phosphatidylinositol 4,5-bisphosphate (PIP2)- and cholesterol-containing monolayers. *Biochemistry.* 48:8241–8248. doi:10.1021/bi9007879

Linck, B., Z. Qiu, Z. He, Q. Tong, D.W. Hilgemann, and K.D. Philipson. 1998. Functional comparison of the three isoforms of the Na+/Ca2+ exchanger (NCX1, NCX2, NCX3). *Am. J. Physiol.* 274:C415–C423.

Lindau, M., and E. Neher. 1988. Patch-clamp techniques for time-resolved capacitance measurements in single cells. *Pflugers Arch.* 411:137–146. doi:10.1007/BF00582306

Liu, Y., L. Casey, and L.J. Pike. 1998. Compartmentalization of phosphatidylinositol 4,5-bisphosphate in low-density membrane domains in the absence of caveolin. *Biochem. Biophys. Res. Commun.* 245:684–690. doi:10.1006/bbrc.1998.8329

Marks, B., and H.T. McMahon. 1998. Calcium triggers calcineurin-dependent synaptic vesicle recycling in mammalian nerve terminals. *Curr. Biol.* 8:740–749. doi:10.1016/S0960-9822(98)70297-0

Miesenböck, G., D.A. De Angelis, and J.E. Rothman. 1998. Visualizing secretion and synaptic transmission with pH-sensitive green fluorescent proteins. *Nature.* 394:192–195. doi:10.1038/28190

Minami, A., and K. Yamada. 2007. Domain-induced budding in buckling membranes. *Eur. Phys. J E Soft Matter.* 23:367–374. doi:10.1140/epje/i2006-10198-5

Newton, A.J., T. Kirchhausen, and V.N. Murthy. 2006. Inhibition of dynamin completely blocks compensatory synaptic vesicle endocytosis. *Proc. Natl. Acad. Sci. USA.* 103:17955–17960. doi:10.1073/pnas.0606212103

Ohtani, Y., T. Irie, K. Uekama, K. Fukunaga, and J. Pitha. 1989. Differential effects of alpha-, beta- and gamma-cyclodextrins on human erythrocytes. *Eur. J. Biochem.* 186:17–22. doi:10.1111/j.1432-1033.1989.tb15171.x

Pavoine, C., and F. Pecker. 2009. Sphingomyelinases: their regulation and roles in cardiovascular pathophysiology. *Cardiovasc. Res.* 82:175–183. doi:10.1093/cvr/cvp030

Ramu, Y., Y. Xu, and Z. Lu. 2007. Inhibition of CFTR Cl- channel function caused by enzymatic hydrolysis of sphingomyelin. *Proc. Natl. Acad. Sci. USA.* 104:6448–6453. doi:10.1073/pnas.0701354104

Rosenboom, H., and M. Lindau. 1994. Exo-endocytosis and closing of the fission pore during endocytosis in single pituitary nerve terminals internally perfused with high calcium concentrations. *Proc. Natl. Acad. Sci. USA.* 91:5267–5271. doi:10.1073/pnas.91.12.5267

Sandvig, K., M.L. Torgersen, H.A. Raa, and B. van Deurs. 2008. Clathrin-independent endocytosis: from nonexisting to an extreme degree of complexity. *Histochem. Cell Biol.* 129:267–276. doi:10.1007/s00418-007-0376-5

Sarasij, R.C., S. Mayor, and M. Rao. 2007. Chirality-induced budding: a raft-mediated mechanism for endocytosis and morphology of caveolae? *Biophys. J.* 92:3140–3158. doi:10.1529/biophysj.106.085662

Schuber, F., K. Hong, N. Düzgünes, and D. Papahadjopoulos. 1983. Polyamines as modulators of membrane fusion: aggregation and fusion of liposomes. *Biochemistry.* 22:6134–6140. doi:10.1021/bi00295a015

Shen, C., M.J. Lin, A. Yaradanakul, V. Lariccia, J.A. Hill, and D.W. Hilgemann. 2007. Dual control of cardiac Na+ Ca2+ exchange by PIP(2): analysis of the surface membrane fraction by extracellular cysteine PEGylation. *J. Physiol.* 582:1011–1026. doi:10.1113/jphysiol.2007.132720

Smillie, K.J., and M.A. Cousin. 2005. Dynamin I phosphorylation and the control of synaptic vesicle endocytosis. *Biochem. Soc. Symp.* 72:87–97.

Smith, C., and E. Neher. 1997. Multiple forms of endocytosis in bovine adrenal chromaffin cells. *J. Cell Biol.* 139:885–894. doi:10.1083/jcb.139.4.885

Song, B.D., M. Leonard, and S.L. Schmid. 2004. Dynamin GTPase domain mutants that differentially affect GTP binding, GTP hydrolysis, and clathrin-mediated endocytosis. *J. Biol. Chem.* 279:40431–40436. doi:10.1074/jbc.M407007200

Staneva, G., A. Momchilova, C. Wolf, P.J. Quinn, and K. Koumanov. 2009. Membrane microdomains: role of ceramides in the maintenance of their structure and functions. *Biochim. Biophys. Acta.* 1788:666–675. doi:10.1016/j.bbamem.2008.10.026

Stefan, C.J., A. Audhya, and S.D. Emr. 2002. The yeast synaptojanin-like proteins control the cellular distribution of phosphatidylinositol (4,5)-bisphosphate. *Mol. Biol. Cell.* 13:542–557. doi:10.1091/mbc.01-10-0476

Takahashi, A., P. Camacho, J.D. Lechleiter, and B. Herman. 1999. Measurement of intracellular calcium. *Physiol. Rev.* 79:1089–1125.

Tam, C., V. Idone, C. Devlin, M.C. Fernandes, A. Flannery, X. He, E. Schuchman, I. Tabas, and N.W. Andrews. 2010. Exocytosis of acid sphingomyelinase by wounded cells promotes endocytosis and plasma membrane repair. *J. Cell Biol.* 189:1027–1038. doi:10.1083/jcb.201003053

Thomas, P., A.K. Lee, J.G. Wong, and W. Almers. 1994. A triggered mechanism retrieves membrane in seconds after Ca^{2+}-stimulated exocytosis in single pituitary cells. *J. Cell Biol.* 124:667–675. doi:10.1083/jcb.124.5.667

Togo, T., J.M. Alderton, G.Q. Bi, and R.A. Steinhardt. 1999. The mechanism of facilitated cell membrane resealing. *J. Cell Sci.* 112:719–731.

Tomita, M., R. Taguchi, and H. Ikezawa. 1983. Adsorption of sphingomyelinase of Bacillus cereus onto erythrocyte membranes. *Arch. Biochem. Biophys.* 223:202–212. doi:10.1016/0003-9861(83)90586-6

Vogel, S.S., R.M. Smith, B. Baibakov, Y. Ikebuchi, and N.A. Lambert. 1999. Calcium influx is required for endocytotic membrane retrieval. *Proc. Natl. Acad. Sci. USA.* 96:5019–5024. doi:10.1073/pnas.96.9.5019

Wang, T.M., and D.W. Hilgemann. 2008. Ca-dependent nonsecretory vesicle fusion in a secretory cell. *J. Gen. Physiol.* 132:51–65. doi:10.1085/jgp.200709950

Wu, X.S., B.D. McNeil, J. Xu, J. Fan, L. Xue, E. Melicoff, R. Adachi, L. Bai, and L.G. Wu. 2009. Ca(2+) and calmodulin initiate all forms of endocytosis during depolarization at a nerve terminal. *Nat. Neurosci.* 12:1003–1010. doi:10.1038/nn.2355

Yan, W., C.M. Jenkins, X. Han, D.J. Mancuso, H.F. Sims, K. Yang, and R.W. Gross. 2005. The highly selective production of 2-arachidonoyl lysophosphatidylcholine catalyzed by purified calcium-independent phospholipase A2gamma: identification of a novel enzymatic mediator for the generation of a key branch point intermediate in eicosanoid signaling. *J. Biol. Chem.* 280:26669–26679. doi:10.1074/jbc.M502358200

Yaradanakul, A., S. Feng, C. Shen, V. Lariccia, M.J. Lin, J. Yang, T.M. Kang, P. Dong, H.L. Yin, J.P. Albanesi, and D.W. Hilgemann. 2007. Dual control of cardiac Na+ Ca2+ exchange by PIP(2): electrophysiological analysis of direct and indirect mechanisms. *J. Physiol.* 582:991–1010. doi:10.1113/jphysiol.2007.132712

Yaradanakul, A., T.M. Wang, V. Lariccia, M.J. Lin, C. Shen, X. Liu, and D.W. Hilgemann. 2008. Massive Ca-induced membrane fusion and phospholipid changes triggered by reverse Na/Ca exchange in BHK fibroblasts. *J. Gen. Physiol.* 132:29–50. doi:10.1085/jgp.200709865

Zha, X., L.M. Pierini, P.L. Leopold, P.J. Skiba, I. Tabas, and F.R. Maxfield. 1998. Sphingomyelinase treatment induces ATP-independent endocytosis. *J. Cell Biol.* 140:39–47. doi:10.1083/jcb.140.1.39